Calreticulin is important for the development of renal fibrosis and dysfunction in diabetic nephropathy

Ailing Lu[a], **Manuel A. Pallero**[a], **Benjamin Y. Owusu**[a], **Anton V. Borovjagin**[a], **Weiqi Lei**[a], **Paul W. Sanders**[b,c] **and Joanne E. Murphy-Ullrich**[a]

***a* - Department of Pathology,** *University of Alabama at Birmingham, Birmingham, AL35294-0019, USA*
***b* - Department of Medicine,** *University of Alabama at Birmingham, Birmingham, AL 35294-0019, USA*
***c* - Department of Veterans Affairs Medical Center,** *Birmingham, AL 35233, USA*

Correspondence to Joanne E. Murphy-Ullrich: *Departments of Pathology, Cell Developmental and Integrative Biology, and Ophthalmology, The University of Alabama at Birmingham, VH G001A/1720 2ND Avenue South, Birmingham, AL 35294-0019, USA. jmurphy@uabmc.edu.*
https://doi.org/10.1016/j.mbplus.2020.100034

Abstract

Previously, our lab showed that the endoplasmic reticulum (ER) and calcium regulatory protein, calreticulin (CRT), is important for collagen transcription, secretion, and assembly into the extracellular matrix (ECM) and that ER CRT is critical for TGF-β stimulation of type I collagen transcription through stimulation of ER calcium release and NFAT activation. Diabetes is the leading cause of end stage renal disease. TGF-β is a key factor in the pathogenesis of diabetic nephropathy. However, the role of calreticulin (*Calr*) in fibrosis of diabetic nephropathy has not been investigated. In current work, we used both in vitro and in vivo approaches to assess the role of ER CRT in TGF-β and glucose stimulated ECM production by renal tubule cells and in diabetic mice. Knockdown of *CALR* by siRNA in a human proximal tubular cell line (HK–2) showed reduced induction of soluble collagen when stimulated by TGF-β or high glucose as compared to control cells, as well as a reduction in fibronectin and collagen IV transcript levels. CRT protein is increased in kidneys of mice made diabetic with streptozotocin and subjected to uninephrectomy to accelerate renal tubular injury as compared to controls. We used renal-targeted ultrasound delivery of Cre-recombinase plasmid to knockdown specifically CRT expression in the remaining kidney of uninephrectomized $Calr^{fl/fl}$ mice with streptozotocin-induced diabetes. This approach reduced CRT expression in the kidney, primarily in the tubular epithelium, by 30–55%, which persisted over the course of the studies. Renal function as measured by the urinary albumin/creatinine ratio was improved in the mice with knockdown of CRT as compared to diabetic mice injected with saline or subjected to ultrasound and injected with control GFP plasmid. PAS staining of kidneys and immunohistochemical analyses of collagen types I and IV show reduced glomerular and tubulointerstitial fibrosis. Renal sections from diabetic mice with CRT knockdown showed reduced nuclear NFAT in renal tubules and treatment of diabetic mice with 11R-VIVIT, an NFAT inhibitor, reduced proteinuria and renal fibrosis. These studies identify ER CRT as an important regulator of TGF-β stimulated ECM production in the diabetic kidney, potentially through regulation of NFAT-dependent ECM transcription.

Introduction

Multiple factors in the diabetic milieu induce endoplasmic reticulum (ER) stress, including oxidative stress, proteinuria, hyperglycemia, advanced glycation end products, and decreased ER calcium stores [1–5]. ER stress has been linked to diabetic complications including atherosclerosis and diabetic nephropathy [4,6–8]. Conditions that induce ER stress often induce increased protein expression and the demand for chaperone-assisted protein folding [4]. Cells respond to ER stress by induction

of the unfolded protein response (UPR), which reduces translation and increases chaperone expression to ensure proper protein folding. In the UPR, ER chaperones, such as glucose response protein 78 (GRP78) and calreticulin (CRT), are upregulated. In the short term, ER stress is adaptive by promoting proper protein synthesis and protecting cells from rises in cytosolic Ca^{2+}, oxidative stress, and cell death [9]. In contrast, chronic ER stress can be pro-apoptotic and pro-inflammatory with loss of function: important new evidence links chronic ER stress with fibrotic disease [1,10–15]. ER stress can augment TGF-β signaling, whereas agents that reduce ER stress attenuate fibrosis [14,16–18]. In the kidney, ER stress affects both epithelial and fibroblast compartments and induces apoptosis, mesenchymal phenotype transition, and alters extracellular matrix (ECM) production by tubular epithelium: this is significant since tubular injury is a major determinant of progressive chronic kidney disease [11,19–21]. ER stress induces renal tubular apoptosis in streptozotocin (STZ)-treated rats and blocking ER stress using a chemical chaperone sodium 4-phenylbutyrate (4-PBA) reduces fibrosis and urinary albumin in diabetic rats [6,9].

CRT is a 46 kDa ER chaperone for N-linked glycoproteins in the CRT/calnexin UPR cycle and a regulator of ER Ca^{2+} homeostasis through its C-terminal Ca^{2+}-binding domain [22,23]. Cell surface CRT mediates apoptotic cell clearance, cellular deadhesion, and migration [24–29]. Purified exogenous CRT stimulates wound healing, suggesting that extracellular CRT also regulates ECM, in addition to its role in ER calcium regulation and chaperone function [30–32]. CRT has effects on the ECM and cellular responses to the ECM and in contrast to exogenous CRT, there is increasing evidence that ER CRT plays a role in fibrogenesis [33]. Fibroblasts overexpressing CRT have increased fibronectin mRNA, protein, and matrix and conversely, while cells lacking CRT express less fibronectin [34,35]. We showed that ER CRT regulates type I collagen expression, processing, and ECM deposition through both chaperone and Ca^{2+} regulatory roles [36]. CRT regulation of Ca^{2+}-dependent c-Src and calmodulin dependent protein kinase II modulates cell adhesion, focal adhesions, vinculin, and fibronectin production [34,35]. CRT overexpression induces epithelial to mesenchymal transition (EMT) in MDCK cells via Ca^{2+}-dependent regulation of Slug and increased expression of collagens and Notch pathway activation in cardiac fibroblasts [37,38]. CRT is also required for TGF-β induced EMT in mouse embryonic stem cells during cardiogenesis and in lung cancer cells [39,40]. In embryoid bodies from CRT null mice, TGF-β receptors were diminished, as was TGF-β-dependent Akt activation, with a resultant increase in GSK3β activity that maintains E-cadherin levels to prevent EMT [39]. Studies document pro-fibrotic effects of CRT on Human Kidney (HK)-2 cells, a human proximal tubular epithelial cell line, in vitro and in vivo [41], consistent with our findings that CRT-regulated NFAT controls ECM transcription in response to TGF-β [20]. We recently showed that tissue specific downregulation of CRT expression in the carotid arteries of *Calr*$^{fl/fl}$ mice attenuates vascular remodeling and reduces neointimal collagen deposition following acute vascular injury [42].

CRT expression is upregulated by cellular and ER stresses, amino acid deprivation, depletion of intracellular Ca^{2+} stores, heat shock, oxidative stress, and hypoxia [43–47]. CRT is associated with fibrotic diseases: elevated CRT levels correlate with fibrosis in rodent models of lung and renal fibrosis, in diabetic atherosclerosis, and in human chronic kidney transplant rejection [7,48,49]. TGF-β increases CRT expression by HK-2 cells, suggesting a feed forward regulation between CRT and TGF-β [48]. CRT is increased in renal interstitial fibroblasts isolated from fibrotic kidneys as compared to fibroblasts from normal kidneys [50]. CRT overexpression by renal proximal tubular cells (LLC-PK1) protects against toxin-induced cell death and oxidative stress [9], but CRT overexpression induces EMT in MDCK cells via Ca^{2+}-dependent regulation of Slug [37]. Mice heterozygous for CRT are protected from tubulointerstitial fibrosis in the unilateral ureteric obstruction model and CRT overexpression in HK-2 cells downregulates epithelial markers and increases FN and collagen IV, confirming an important role for CRT in renal fibrosis and tubular repair responses [41]. Although CRT has not been identified as a biomarker for diabetic nephropathy through human urinary proteomic or GWAS approaches, there is evidence that CRT expression is increased in mononuclear cells from patients with type 2 diabetes and in adipose tissue from obese, insulin resistant individuals and that *CALR* transcript and protein are increased in leukocytes isolated from healthy individuals following a glucose challenge [51–53]. Interestingly, CRT has been identified as an aging associated frailty biomarker [54].

High glucose upregulates CRT by multiple cell types, including endothelial cells, vascular smooth muscle cells, HepG2 cells, mouse embryonic fibroblasts, and L6 skeletal muscle cells through PPARδ [55,56] and hexosamine pathways [57,58]. CRT is increased in diabetic arteries and the chemical chaperone 4-PBA reduces CRT expression [7]. CRT is also increased in diabetic retina, in glucose treated zebrafish cardiomyocytes, and in rat diabetic cardiomyopathy [18,59,60]. ER chaperones are increased in biopsies of human diabetic kidneys and CRT is expressed in both glomeruli and tubules in normal and diabetic kidneys [1]. A recent report shows elevated CRT levels in kidney lysates from type 2 diabetic *db/db* mice and in a human proximal

tubular epithelial cell line (HK-2) following glucose treatment [61]. In these in vitro studies, CRT knockdown reduces epithelial to mesenchymal transition induced by glucose [61]. Despite these findings, the importance of CRT in renal fibrosis in diabetic kidney disease is unknown.

Given the importance of TGF-β for fibrotic remodeling in diabetic nephropathy [62], the increase in ER stress in diabetes, and the role of CRT in regulating fibrotic responses to TGF-β in vitro, we asked whether CRT contributes to fibrosis and renal dysfunction in diabetic nephropathy. To address this question, *Calr*$^{fl/fl}$ mice were subjected to uninephrectomy to accelerate renal disease and then diabetes was induced using STZ [63,64]. Mice were then treated to induce targeted down regulation of CRT expression in the kidney via microbubble (MB)-assisted delivery of Cre-recombinase plasmid followed by renal-targeted ultrasound (US). In diabetic mice, reduced renal expression of CRT attenuated proteinuria and renal fibrosis, collagen I and IV expression, NFAT activation, and improved survival. Furthermore, treatment with the NFAT inhibitor, 11R-VIVIT reduced proteinuria in diabetic mice. Together these data suggest that CRT is an important contributor to renal dysfunction and fibrosis in the diabetic environment.

Results

TGF-β and 30 mM glucose regulate CRT expression by HK-2 cells and knockdown of CRT attenuates stimulation of extracellular matrix production

Previously, we showed that CRT is required for TGF-β stimulation of extracellular matrix production and that knockdown of CRT attenuates TGF-β-dependent transcription of collagen I and fibronectin in fibroblasts and in vascular smooth muscle cells [20,36,42]. Upregulation of CRT has pro-fibrotic effects on a human renal tubular epithelial cell line (HK-2) and TGF-β stimulates CRT expression by these cells [41,48]. High glucose levels and oxidative stress associated with diabetes induce TGF-β activity as well as increase CRT expression in multiple cell types, including endothelial cells, vascular smooth muscle cells, HepG2 cells, mouse embryonic fibroblasts, and L6 skeletal muscle cells through PPARδ [55,56] and hexosamine pathways [57,58]. Therefore, we asked whether TGF-β and high glucose stimulate increases in CRT levels in HK-2 cells. First, we showed that knockdown of CRT in HK-2 cells with siRNAs reduced CRT expression by >60% 24 h after transfection, which persisted for over 96 h (Figs. 1A,B). Next, we examined HK-2 cells treated with TGF-β or 30 mM glucose and observed increased CRT protein expression 48–72 h after treatment (Fig. 1B). Consistent with our previous findings that CRT can regulate TGF-β-dependent transcription of FN [20], siRNA CRT knockdown reduced TGF-β and 30 mM glucose stimulation of fibronectin transcript as compared to control HK-2 cells and cells transfected with non-targeting siRNA (Fig. 1C,D). Similarly, CRT siRNA also reduced TGF-β and 30 mM glucose induction of col. IV transcript. For reasons that are not clear, transfection with NT siRNA attenuated TGF-β, but not glucose, stimulation of col. IV transcript. As knockdown of CRT can decrease both collagen expression as well as trafficking and secretion [36], we also measured newly-synthesized, acid-soluble collagens in the conditioned media using the Sircol assay which recognizes the Gly-X-Y helical region of collagens. Both TGF-β and 30 mM glucose stimulate collagen secretion by HK-2 cells and this increased soluble collagen is attenuated by siRNA CRT knockdown in cells with reduced CRT expression (Fig. 1E).

CRT expression is increased in diabetic mouse kidneys

Increased expression of CRT has been observed in the aorta of diabetic hamsters [7]. However, it is not known if CRT expression is also increased in kidneys of diabetic animals. We previously observed increased levels of CRT by Western blotting of renal lysates and by immunohistochemistry in kidneys from Akita mice with type 1 diabetes (unpublished data). In current studies, we compared CRT expression in kidneys from approximately 15 week old control *Calr*$^{fl/fl}$ mice with those of streptozocin-treated uni-nephrectomized *Calr*$^{fl/fl}$ diabetic mice of similar age. Staining of renal sections from diabetic *Calr fl/fl* mice showed an increase in CRT in the tubules and glomeruli as compared to control mice (Fig. 2).

Knockdown CRT in kidneys of streptozotocin-treated diabetic mice through use of Cre-recombinase plasmid delivered by ultrasound with microbubbles

In our previous studies, we used MB in conjunction with targeted US for selective delivery of Cre-recombinase plasmid to knockdown CRT expression in specifically ligated carotid arteries of *Calr*$^{fl/fl}$ mice [42]. Using a similar approach, in these current studies, we used renal-targeted US to deliver plasmid expressing Cre-recombinase-IRES-GFP or a control GFP plasmid to uni-nephrectomized, streptozoctin-treated diabetic *Calr*$^{fl/fl}$ mice. In pilot studies, we observed that a single bolus of Cre-recombinase plasmid/MB mixture reduced CRT protein levels in US-targeted mouse kidneys. Western blotting of renal lysates and immunohistochemical analyses of renal

sections stained with anti-CRT antibodies showed decreased CRT protein in kidneys at days 2, 7, and 14 post-treatment with significance by day 7 (Supplemental Fig. 1a,b). As acute kidney injury can predispose to later chronic kidney injury, we also wanted to assess whether the MB/US protocol might induce acute kidney injury [65]. Therefore we measured urinary Kim-1, a sensitive urinary marker of acute kidney tubule injury (KIM-1) which is rapidly upregulated 5-fold within 24 h following various types of injury [66,67]. Urinary Kim-1 increased only slightly two days after treatment with US at 0.7 mPa peak negative pressure (6598 pg/ml treated vs 2857 pg/ml control), independent of plasmid delivery and calreticulin levels. The albumin/creatinine ratio in urines obtained 14 days after treatment with Cre-

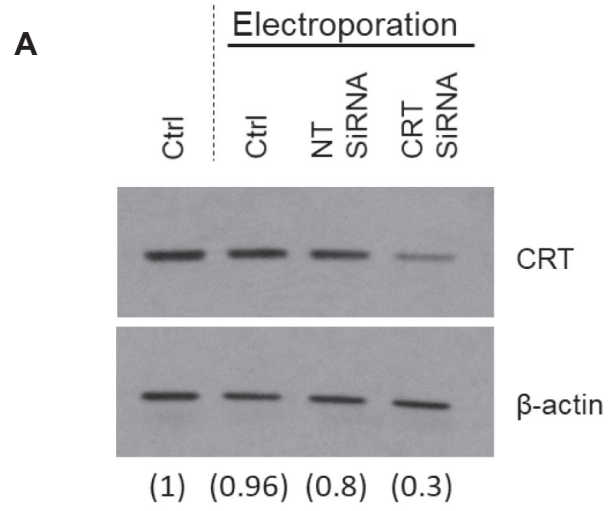

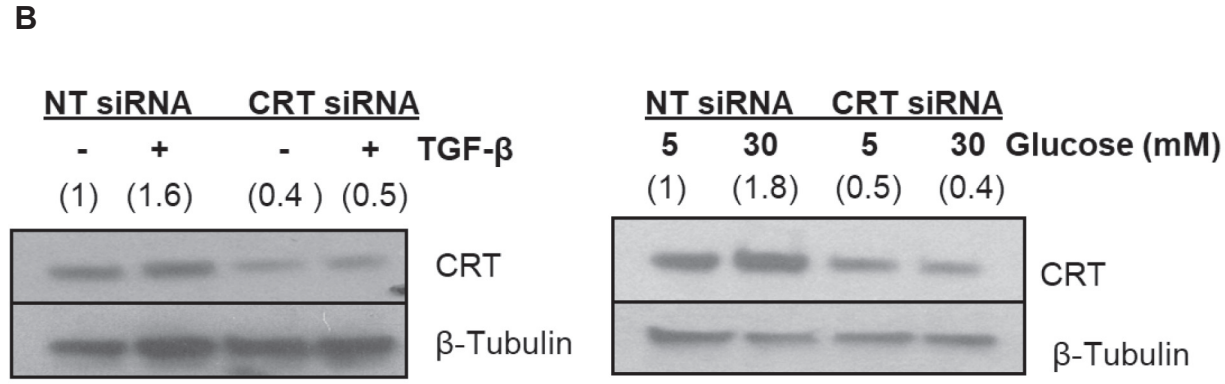

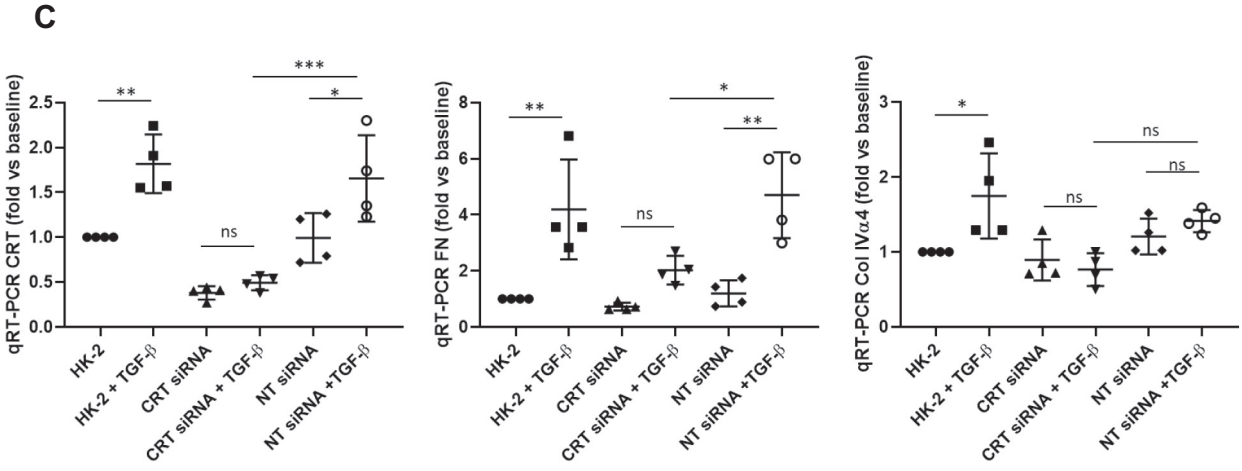

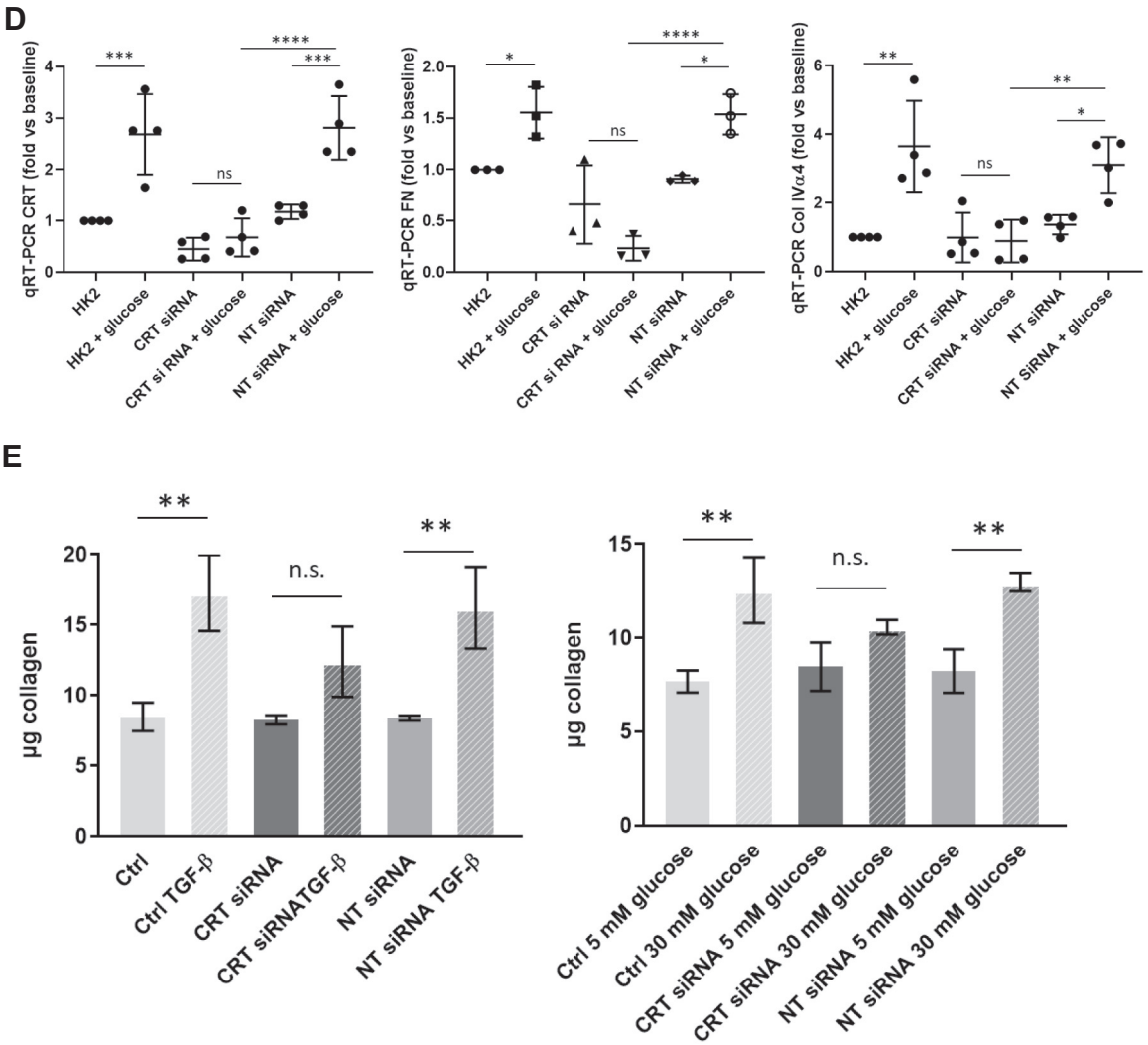

Fig. 1. HK-2 cells treated with TGF-beta or glucose: CRT levels; siRNA effect on collagen I, IV and fibronectin (FN). 1A) HK-2 cells were transfected with either non-targeting or CRT-targeting pools of siRNAs and incubated overnight in complete media. Media was changed and cells incubated for another 24 h prior to harvest with Laemmli buffer. CRT was normalized to β-actin as a loading control and results compared to control cells or cells subjected to electroporation without siRNA. Relative protein expression (shown in parentheses) was calculated relative to protein levels in non-transfected, non-electroporated cells (Ctrl). 1B, C) HK-2 cells were transfected and incubated in medium for 24 h and then treated with B) TGF-β (350 pM) or C) 5 or 30 mM glucose in media with 2% FBS for 72 h. Cell extracts were evaluated for CRT and results were normalized to β-tubulin as a loading control. Relative protein expression (shown in parentheses) was calculated relative to protein levels in untreated non-targeting (NT) siRNA transfected cells. Results are representative of multiple experiments. 1D) HK-2 cells were transfected with either non-targeting or CRT-targeting pools of siRNAs and incubated overnight in complete media. Media was changed and cells incubated for 24 h further in media with 2% FBS. Cells were then treated with TGF-β (350 pM) for 24 h or with 5 or 30 mM glucose for 72 h. RNA was harvested and qRT-PCR run for *calr, fn*, and *collVα4* as described in the methods. Data were analyzed using the ΔΔCt method with S9 used for normalization. Data are normalized to untreated HK-2 cells. Results are means ± SD of 3–4 separate experiments. Data were analyzed by one-way ANOVA with Tukey's post-hoc analysis or Dunnett's multiple comparison testing (FN, HK-2 vs HK-2 + Glucose). *$p < 0.05$; **$p = 0.001$ to 0.01; ***$p = 0.0001$ to 0.001; ****$p < 0.00001$ 1E) Soluble collagens in the conditioned media of HK-2 cells were quantified by the Sircol™ assay after 72 h of treatment with either TGF-β (350 pM) or 5 or 30 mM glucose. Treatments were initiated ~42 h following transfection with non-targeting (NT) or *calr* targeting siRNA (CRT siRNA). Results are the means ± SEM from 3 separate experiments. Control vs control TGF-β **$p = 0.0015$; NT siRNA vs NT siRNA TGF-β **$p = 0.0038$, CRT siRNA vs CRT siRNA TGF-β n.s.; control 5 mM glucose vs 30 mM glucose **$p = 0.0013$; NT siRNA 5 mM glucose vs NT siRNA 30 mM glucose **$p = 0.0016$; CRT siRNA 5 mM glucose vs CRT siRNA 30 mM glucose, n.s. Analysis was performed using one way ANOVA with Tukey's post-hoc analysis. CRT knockdown was confirmed by immunoblotting (data not shown).

Fig. 2. CRT expression is increased in uninephrectomized diabetic kidneys. Kidneys of control and streptozotocin-treated, uninephrectomized diabetic kidneys of *Calr*$^{fl/fl}$ mice were stained for CRT with rabbit monoclonal anti-CRT antibody. Staining was quantified in six different 10× fields in 4 animals/group. Results are the means ± SEM. ***$p < 0.0002$, analyzed by the two-tailed unpaired *t*-test. Original magnification 40×.

recombinase plasmid with MB/US was not different from that of urines from mice treated with Cre-recombinase plasmid alone without MB/US (Cre plasmid MB/US 12.6 μg/mg ACR vs Cre plasmid 10.8 μg/mg ACR). Together, these studies suggest that the MB/US treatment itself does not cause demonstrable acute kidney injury, demonstrating the feasibility of using this in vivo approach to specifically knockdown CRT expression in mouse kidneys.

Knockdown of CRT in diabetic kidneys reduces proteinuria and improves survival

Calr$^{fl/fl}$ mice were made diabetic by treatment with streptozotocin and renal tubular injury was accelerated by uni-nephrectomy [63,64]. Two weeks following nephrectomy, mice were subjected to low dose streptozotocin treatment for 5 days. Two weeks later, induction of diabetes was confirmed by measuring blood glucose levels (data not shown). Mice were then subjected to 0.7 Mpa pressure US at 1 MHz frequency of ultrasound with systemic plasmid/MB delivery via tail vein injection on days 1 and 22. Studies were continued for a total of 22 weeks. In kidneys harvested both at 14–16 and at 22 weeks, CRT levels detected by Western blot analyses of renal lysates (Fig. 3A) or by immunohistochemical staining (Fig. 3B) showed that knockdown of CRT to approximately 60–70% of those in control (GFP) plasmid or untreated diabetic mice persisted over the course of these studies.

Urinary albumin and creatinine were measured to determine the effects of CRT knockdown on renal function in diabetic mice. In urines collected during early disease at 5–7 weeks following ultrasound plasmid/MB delivery, Cre-recombinase plasmid-treated mice showed reduced urinary albumin and albumin/creatinine ratio as compared to GFP plasmid-treated diabetic mice (Fig. 4A). Importantly, in later disease, urines from mice treated with Cre-recombinase plasmid collected 17–19 weeks following plasmid delivery, showed significantly reduced urinary albumin and albumin/creatinine ratio as compared to either saline or GFP plasmid treated controls (Fig. 4B). Urinary albumin and albumin/creatinine ratio do not differ between saline-treated diabetic mice and GFP MB/US treated diabetic mice at either 5–7 or 17–19 weeks. Interestingly, diabetic mice treated with Cre-recombinase plasmid trended towards improved survival as compared to diabetic control mice ($p = 0.06$) over the course of these studies (Fig. 4C).

CRT knockdown reduces renal fibrosis in diabetic mice

Consistent with the observed reduction in TGF-β- or glucose-stimulated collagen expression and secretion in a human proximal tubular cell line with CRT knockdown, kidneys from diabetic mice with CRT knockdown showed reduced renal fibrosis/mesangial expansion in contrast to diabetic mice from Saline and GFP MB/US groups that have glomerular and tubulointerstitial fibrosis, characteristic of diabetic nephropathy. PAS staining was reduced by nearly 50% in glomeruli from diabetic mice treated with Cre-recombinase as compared to saline or GFP control plasmid-treated diabetic mice (Fig. 5A). Qualitative electron microscopic examination also showed reduced tubulointerstitial fibrosis, foot process effacement, and glomerular basement membrane thickening in Cre-recombinase plasmid MB/US treated diabetic mice as compared to GFP plasmid MB/US treated diabetic mice (Fig. 5B).

Immunohistochemical staining for collagen type I was significantly decreased (by ~70%) in diabetic kidneys with reduced CRT expression, particularly in the tubular interstitium (Fig. 5C). As thickening of the glomerular basement membrane with increased collagen type IV is characteristic of diabetic kidney disease, we assessed the effect of CRT knockdown on type IV collagen in diabetic kidneys [68,69]. Type IV collagen staining was similarly reduced by ~50% in both the glomerular area and in the overall cortical region in kidneys from mice with CRT knockdown (Fig. 5C).

Our previous studies in mouse embryonic fibroblasts showed that Smad phosphorylation was not compromised in TGF-β-stimulated CRT-null cells [20], although other studies have reported a correlation between reduced Smad phosphorylation with reduced or absent CRT expression [40,41]. In our studies, we did not observe any reduction in phosphorylated Smad 2 in kidneys with CRT knockdown (data not shown).

CRT knockdown reduces active NFAT and blocking NFAT reduces renal fibrosis

CRT-mediated release of ER calcium increases activation of NFAT [23,70]. Previously, we showed that CRT-dependent NFAT activation is required for TGF-β stimulation of collagen and fibronectin transcription [20]. Given that NFAT plays a role in extracellular matrix production in diabetic tissues [71–74], we examined whether knockdown of CRT in diabetic kidneys reduced NFAT activity. Indeed, there was a significant reduction in staining of nuclear NFAT, an indicator of NFAT activity, in tubular epithelium of diabetic kidneys treated with Cre-recombinase plasmid to reduce CRT expression (Fig. 6). Because the cell permeable NFAT inhibitor, 11R-VIVIT, has been shown to reduce glomerulosclerosis, albuminuria, and podocyte apoptosis in the *db/db* model of type 2 diabetes [73], we asked whether 11R-VIVIT has similar protective effects on renal function in this model of type 1 diabetes. 11R-VIVIT is a selective inhibitor of

calcineurin-mediated NFAT dephosphorylation and unlike other calcineurin inhibitors such as cyclosporine A and tacrolimus, which are associated with nephrotoxicity and increased TGF-β signaling, 11R-VIVIT does not block NFAT-independent calcineurin interactions with other proteins and engagement in other signaling pathways [75,76]. Uninephrectomized, streptozotocin-treated *Calr*$^{fl/fl}$ mice were treated with intraperitoneal injection of 11R-VIVIT for 11 weeks. Mice treated with 11R- VIVIT showed

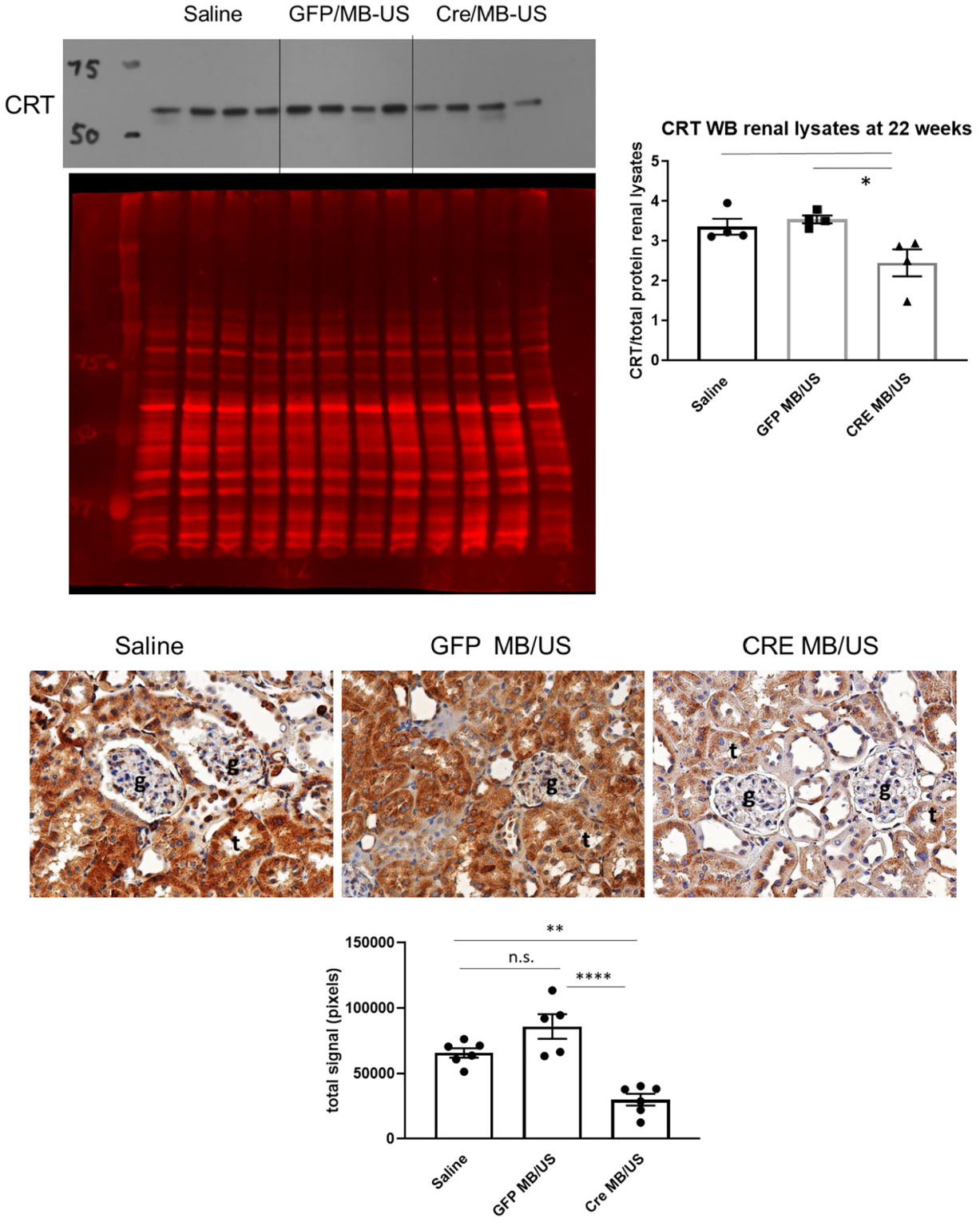

decreased albuminuria and albumin/creatinine ratio in this model of type 1 diabetes (Fig. 7A). PAS staining in glomeruli was also reduced (Fig. 7B). Together, these data establish that NFAT is an important factor in the development of renal dysfunction and fibrosis in a model of type 1 diabetes in which reduction of CRT expression is protective.

Discussion

These studies identify CRT as an essential mediator of the induction of renal fibrosis and dysfunction in a model of type 1 diabetes with uninephrectomy. Mice with stably reduced renal expression of CRT had improved renal function and survival and reduced active NFAT and fibrosis. In vitro studies showed that knockdown of CRT in a human proximal tubule cell line attenuated the ability of high glucose or TGF-β to stimulate fibronectin and type I collagen at the protein level, fibronectin and type IV collagen expression at the mRNA transcript level, and reduced secretion of soluble collagens.

As global knockout of *calr* results in embryonic lethality, it has been difficult to assess the functional role of CRT in disease models [70]. Other investigators have successfully used *calr* heterozygous mice to identify a role for CRT in various fibrotic diseases other than diabetes [41,48]. In these current studies, we examined the effects of *calr* knockdown in adult animals following disease induction to avoid any developmental effects that might affect cellular responses to injury and possibly confound responses. Furthermore, *calr* knockdown was targeted to the kidney to avoid systemic influences from global *calr* knockdown. This approach using tissue targeted ultrasound targeted delivery of Cre-recombinase plasmid to $calr^{fl/fl}$ mice was successfully used in our previous studies to examine the role of CRT in mediating neointima formation following acute carotid injury [42]. Importantly, knockdown persisted during the 22 week course of these renal studies. Furthermore, MB/US treatment did not acutely induce significant levels of urinary KIM-1, a marker of acute kidney injury [77]: this is important since acute kidney injury can pre-dispose to later chronic kidney disease [65]. In addition, urinary albumin and the ACR in both early and late disease did not differ between saline and GFP MB/US treated groups, suggesting that this treatment in itself did not significantly affect acute or chronic renal function. Rather, differences in renal function and fibrosis are likely due to knockdown of CRT expression. Although CRT expression was most obviously decreased in the tubules as assessed by IHC, our knockdown strategy likely impacts the entire nephron and these studies showed that CRT knockdown attenuated both glomerular and proximal tubular injury in this model of diabetes.

CRT affects both TGF-β dependent transcriptional regulation of ECM molecules through NFAT and trafficking/secretion of fibrillar type I collagen in fibroblasts [20,36]. These current studies show that CRT similarly regulates ECM transcript, protein, and levels of soluble collagens in cultured HK-2 cells stimulated with either glucose or TGF-β. This diabetic model provides evidence of decreased collagen I and IV in tissues with CRT downregulation, which could result from a combination of reduced transcription and protein secretion/ECM assembly. These studies suggest that there might be cell type specific differences in how CRT regulates TGF-β signaling as we did not observe any defects in Smad phosphorylation or nuclear import in diabetic renal tissues in our current studies or in TGF-β-treated CRT null MEFs. In contrast, in CRT null embryoid bodies, TGF-β receptors levels are diminished, which would be expected to result in decreased Smad activity [20,39].

Given the importance of calcineurin/NFAT signaling in diabetes and for response to TGF-β and the downregulation of activated NFAT in renal tubules of mice with *calr* knockdown, it is also likely that CRT mediates diabetic renal fibrosis through NFAT-dependent transcription, as well as, via regulation of ECM trafficking/secretion [71,72,78]. Furthermore, our studies show that the NFAT inhibitor, 11R-VIVIT reduces renal fibrosis in this model of type 1 diabetes, consistent with the known roles for NFAT in type 2 diabetic nephropathy and in glomerulosclerosis, podocyte injury, mesangial cell ECM production, and tubular apoptosis [73,74,79,80].

CRT destabilizes glucose transporter 1 mRNA in vascular smooth muscle cells under high glucose conditions and CRT deficient cells have increased insulin receptor density, glucose transporter-1, and insulin signaling [55,81]. Although no differences in blood glucose levels between STZ-treated saline,

Fig. 3. Delivery of Cre-recombinase plasmid with MB/US to kidneys of $Calr^{fl/fl}$ mice reduces calreticulin protein in diabetic uninephrectomized kidneys over 22 weeks. A) Renal lysates of kidneys harvested 22 weeks after the first injection of plasmids were evaluated for calreticulin protein by immunoblotting. Protein concentration from RIPA buffer lysates was determined by BCA protein assay and results are normalized to total protein loaded as determined using the REVERT total protein stain. Results are the means ± SEM, $^{*}p = 0.044$ for Saline vs Cre MB/US and $^{*}p = 0.026$ for GFP MB/US vs Cre MB/US $^{*}p = 0.026$, using one way ANOVA with Holm-Sidak post-hoc analysis. B) Immunohistochemical staining for calreticulin in kidneys at 22 weeks was evaluated in fifteen 10× sections/animal (n = 5–6 animals/group). (g), glomerulus; (t) tubules; Saline vs Cre MB/US, $^{**}p = 0.0016$, GFP MB/US vs Cre MB/US, $^{****}p < 0.0001$ by one way ANOVA with Tukey's post-hoc analysis.

GFP MB/US, and CRE MB/US groups were observed in our studies (data not shown), it is possible that there are local differences in glucose metabolism and insulin signaling in Cre-recombinase treated kidneys with lower CRT levels that might also contribute to improved survival of the diabetic animals.

Other chaperones such as BiP (GRP78) and HSP47 have also been implicated in fibrosis and collagen trafficking [33,82–86]. The fact that these chaperones were not targeted in these studies, suggests that the major role for CRT in diabetic nephropathy-related fibrosis is upstream of ECM chaperone/trafficking, likely through NFAT-dependent transcription. CRT differs from most other chaperones, because of its ability to regulate ER calcium release to activate calcinuerin leading to NFAT dephosphorylation and activation [22]. Agents that attenuate ER stress/the unfolded protein response, such as the bile acid tauroursodeoxycholic

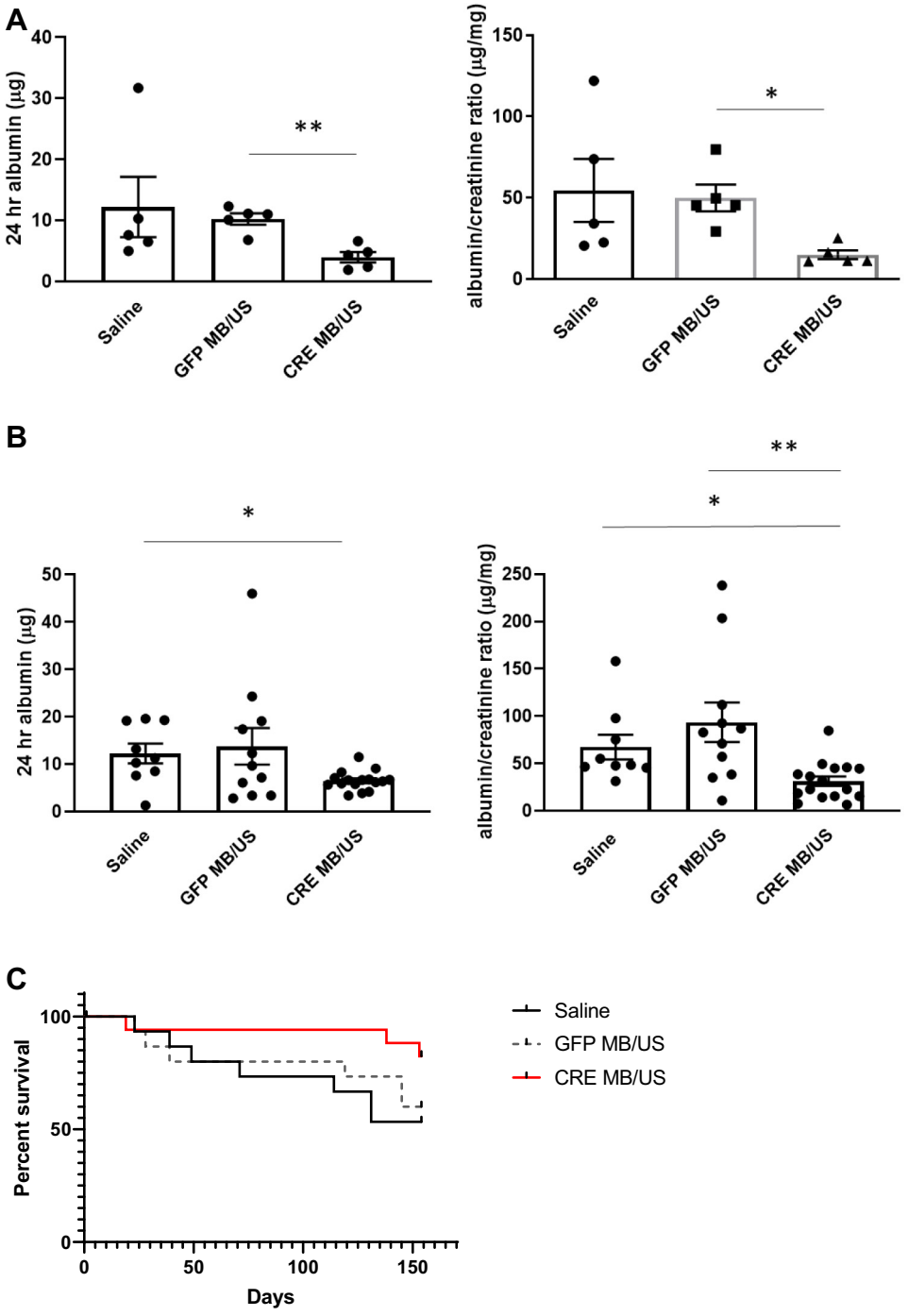

acid [14] and 4-phenylbutyrate [16], have been shown to reduce fibrosis in several pre-clinical models of ER stress triggered fibrosis. Given the multiple critical functions of CRT in both intracellular and extracellular compartments [22,32,87], direct targeting of CRT might be therapeutically challenging [88]. Our data suggest that NFAT antagonists represent another approach to controlling fibrosis in diseases with upregulated CRT expression.

Methods

GFP and Cre-recombinase plasmid constructs

pCAG-Cre-IRES2-GFP (Plasmid #26646) was purchased from Addgene (Watertown, MA). GFP plasmid was purchased from Invitrogen (Madison, WI). Plasmids were isolated from *E. coli* and purified using a Qiagen EndoFree Plasmid Giga Kit (Cat 12,391) as described previously [42].

siRNAs

A pool of 4 different human CALR siRNAs (L-008197-00-0005, ON-TARGET plus Human CALR (811) siRNA– SMARTpool) were used for the HK-2 transfection studies (Dharmacon, Lafayette, CO). ON-TARGET plus Non-targeting siRNA #1 was also purchased from Dharmacon. Sequences of individual siRNAs of the pool used to target CALR are shown:

ON-TARGETplus SMARTpool siRNA J-008197-06,	CALR Target Sequence: CCUAUGAGGUGAAGAUUGA
ON-TARGETplus SMARTpool siRNA J-008197-07,	CALR Target Sequence: GCACGGAGACUCAGAAUAC
ON-TARGETplus SMARTpool siRNA J-008197-08,	CALR Target Sequence: GAAGCUGUUUCCUAAUAGU
ON-TARGETplus SMARTpool siRNA J-008197-09	CALR Target Sequence: GCAAGGAUGAUGAGUUUAC
ON-TARGETplus Non-targeting siRNA D-001810-01-05	Target Sequence: UGGUUUACAUGUCGACUAA

Quantitative RT-PCR

PCR primers were obtained from BIO-RAD (Hercules, CA).

Calreticulin	AGAAATTGACAACCCCGAGTATT
Amplicon Context Sequence	CTCCCGATCCCAGTATCTAT GCCTATGATAACTTTGGCGT GCTGGGCCTGGAC CTCTGGCAGGTCAAGTCTGGCAC CATCTTTGAC AACTTCCTCATCACCAAC GATGAGGCATACGCTGAGG AGTTTGGCAACGAGA
collagen, type IV, α4	GGGCCCTTTTCTCCCTGGAGGTCC
Amplicon Context Sequence	AGGTAAACCCTTCTCTCCA GGTGGCCCAGG AAATCCATGTGGT CCCTGCGGTCCCGGGAATCCCACT GGTCCTTTCTGGCCATC TTTTCCATCACATCCTGGAA AGCCTTTGTATCCTGG
Fibronectin 1	AACGTCCTGCCATTGTAG
Amplicon Context Sequence	GTGAATGGTAAGACACATGGC TCTCCATTTGAGTTGCCACCG TAAGTCTGGGTTACAGC TGTCTCTTGGCAGCTGAC TCCGTTGCCCAGGC ACGTGCAAAGCATTTGCTTATTT CCTTGTGTCTTCAG CCACTGCATCCCCACAGAGTAG
Ribosomal protein S9	CCGCCCGGGAACTGC
Amplicon Context Sequence	TGACGCTTGATGAGAAGGACCCA CGGCGTCTGTTCGAA GGCAACGCCCTGCTGCGGCGGCT GGTCCGCATTGGGGTGCTGGATGA GGGCA AGATGAAGCTGGATTACATCCTGG GCCTGA

Cell culture

HK-2 cells (ATCC® CRL-2190™) were maintained in keratinocyte serum-free media supplemented with bovine pituitary extract and epidermal growth factor (Gibco), 2% fetal bovine serum (Atlanta Biologicals), and penicillin-streptomycin (Gibco) under standard cell culture conditions.

Fig. 4. CRT knockdown reduces renal dysfunction and improves survival in uninephrectomized diabetic mice: 4 A,B) CRT knockdown reduces albuminuria and the albumin/creatinine ratio 24 h urines were collected over weeks 5–7 (panel A) and at weeks 17–19 (panel B) following the first plasmid injection with microbubbles and ultrasound (MB/US), which is 2.5 weeks following the first streptozotocin injection. Urines were analyzed for albumin (panel) and the albumin/creatinine ratio (right panel). Only animals with blood glucose >200 mg/dl were included. Results are the means ± SEM. Panel A: albumin: Welch's ANOVA with Dunnett's T3 multiple comparison's test GFP MB/US vs CRE MB/US $^{**}p = 0.003$; n.s. saline vs GFP or saline vs CRE MB/US, $n = 5$. Albumin/creatinine ratio: One way ANOVA with Dunnett's T3 multiple comparison's test GFP MB/US vs CRE MB/US $^{*}p = 0.026$; n.s. saline vs GFP or saline vs CRE MB/US, n = 5 Panel B: albumin: $^{*}p = 0.038$, one-way ANOVA; albumin/creatinine ratio: Kruskal-Wallis $^{*}p = 0.025$; $^{**}p = 0.004$, $n = 9 = 16$. Saline vs GFP MB/US: not significant for all conditions in Panels A and B. 4C): CRT knockdown improves survival in diabetic uninephrectomized mice. Kaplan-Meier survival curves indicate that survival is trending towards improvement in mice with knockdown of CRT as compared to saline injected control mice; $p = 0.07$, logrank test for trend for 3 groups, $p = 0.18$, logrank mantel-cox for 3 groups; $p = 0.06$ for saline vs Cre-recombinase (two groups), $p = 0.16$ for GFP MB/US vs Cre MB/US (two groups).

Transfection

HK-2 cells (1×10^6) were transfected with 300 nM of either the pooled CRT-specific or non-targeting (NT) siRNA (GE Dharmacon) by nucleofection following Amaxa™ Basic Nucleofector Protocol for Mammalian Epithelial Cells (Lonza, VPI-1005). Nucleofection was achieved using the two pulses of A-023 program on the Nucleofector I Device. Transfected cells were seeded at a density of 2×10^5 cells in 0.5 ml media per well in a 12-well cell culture plate and incubated in a humidified 37 °C, 5% CO_2 incubator overnight. Medium was changed and then further incubated for 24–72 h in media containing 2% fetal bovine serum for the Sircol™ assay or qRT-PCR as described in figure

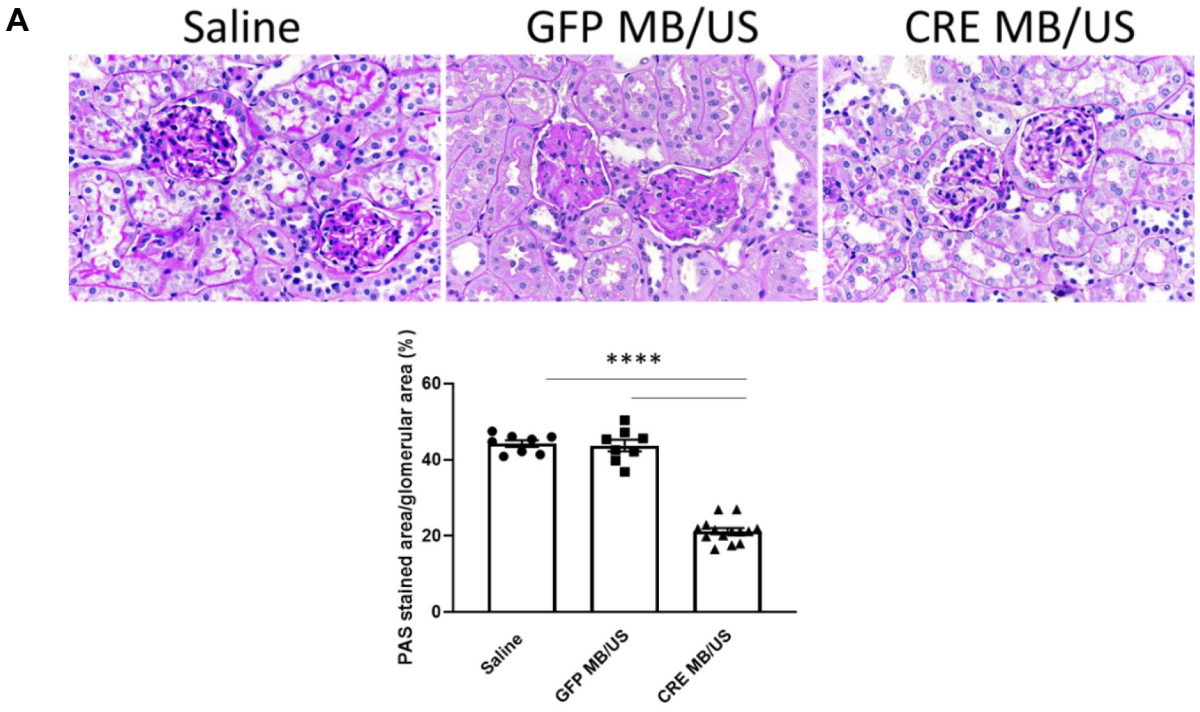

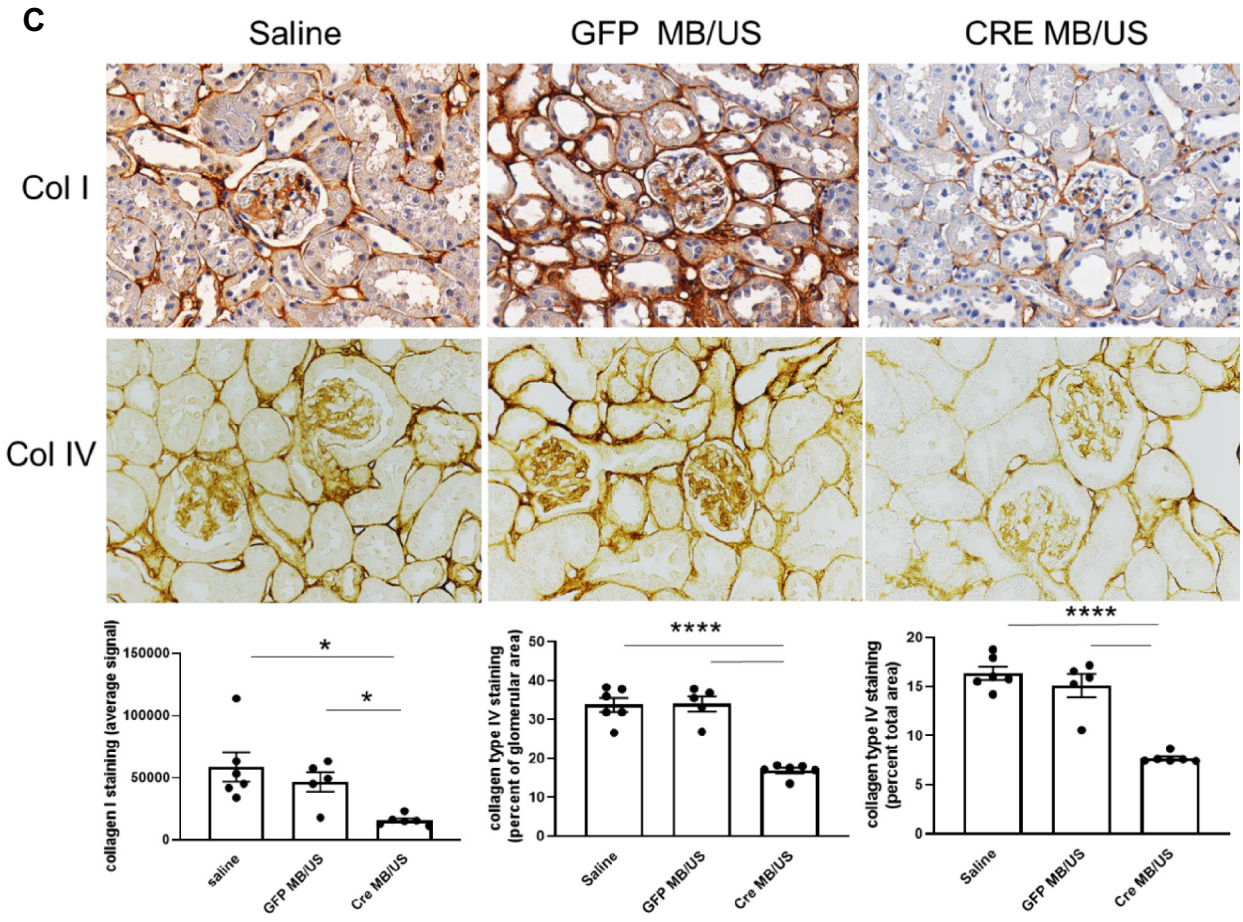

Fig. 5. CRT knockdown reduces fibrosis in kidneys of diabetic mice. 5A) Mice treated with Cre-recombinase plasmid had reduced glomerular PAS staining 22 weeks after the first plasmid injection. (n = 8–14 animals/group, 15 glomeruli/animal). Original magnification was 40×. Results are means ± SEM. By One-way ANOVA with Tukey post-doc analysis, saline vs Cre MB/US and GFP MB/US vs Cre MB/US ****$p < 0.0001$. 5B) Transmission electron micrographs of kidneys from GFP MB/US treated diabetic mice (A-C) and CRE MB/US treated diabetic mice (D-F). Panel A shows fibrillary collagen bundles (blue arrows) in the interstitial space between 2 tubules (t) in GFP MB/US kidney (original magnification 1650×). Panels B and C show thickened glomerular basement membrane (*) and epithelial foot process effacement (red arrows) (B original magnification 3200×; C original magnification 6500×). Images of CRE MB/US treated mice show more normal tubular interstitial space, glomerular basement membranes, and epithelial foot processes (D, original magnification 2100×; E, original magnification 3200×; F original magnification 6500×). 5C) Renal sections were stained with antibody to either type I collagen or type IV collagen (n = 5–6 animals/group, 15 sections or glomeruli/animal) and analyzed for average signal of brown staining per slide (collagen type I) or percent of glomerular area and percent of total area for collagen type IV brown staining. Sections stained with anti-type I collagen were counterstained with hematoxylin. Collagen I staining, *$p = 0.04$, saline vs Cre MB/US and GFP MB/US vs Cre MB/US by one-way ANOVA with Dunnett's T3 multiple comparisons test. For collagen IV staining, ****$p < 0.0001$ for both saline vs Cre MB/US and GFP MB/US vs Cre MB/US by one-way ANOVA with Tukey's post-hoc analysis.

legends. CRT knockdown was confirmed by immunoblotting and qRT-PCR.

TGF-β and glucose treatment

On the day following transfection, media were removed and replaced with fresh media containing 2% fetal bovine serum and incubated further for 24 h. HK-2 cells were then treated with either 350 pM TGF-β1 (R&D Systems (Cat #240b), Minneapolis, MN) or 5 or 30 mM glucose (Sigma-Aldrich (#G7021), St. Louis, MO) in media with 2% FBS every 24 h for a total period of 24 for TGF-β treatment and for 72 h for glucose treatment.

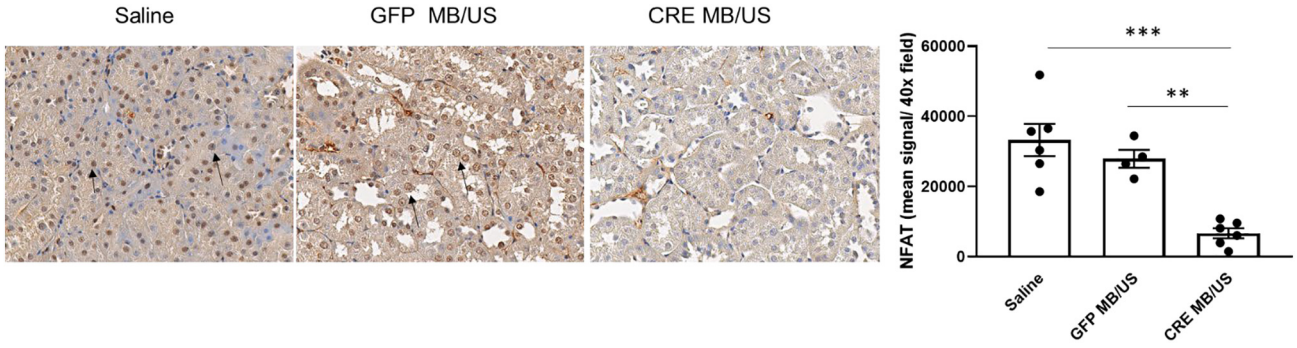

Fig. 6. Renal tubular nuclear NFAT is reduced in diabetic kidneys with CRT knockdown. Renal sections harvested from animals 22 weeks after the first plasmid treatment were stained for NFAT2 (NFATc1) and the mean signal of NFAT staining in fifteen 40× fields/animal was evaluated (n = 4–6 animals/group). Results are the means ± SEM. Saline vs Cr MB/US ***p = 0.0001 and GFP MB/Us vs Cre MB/US **p = 0.002, by one-way ANOVA with Tukey's post-hoc analysis.

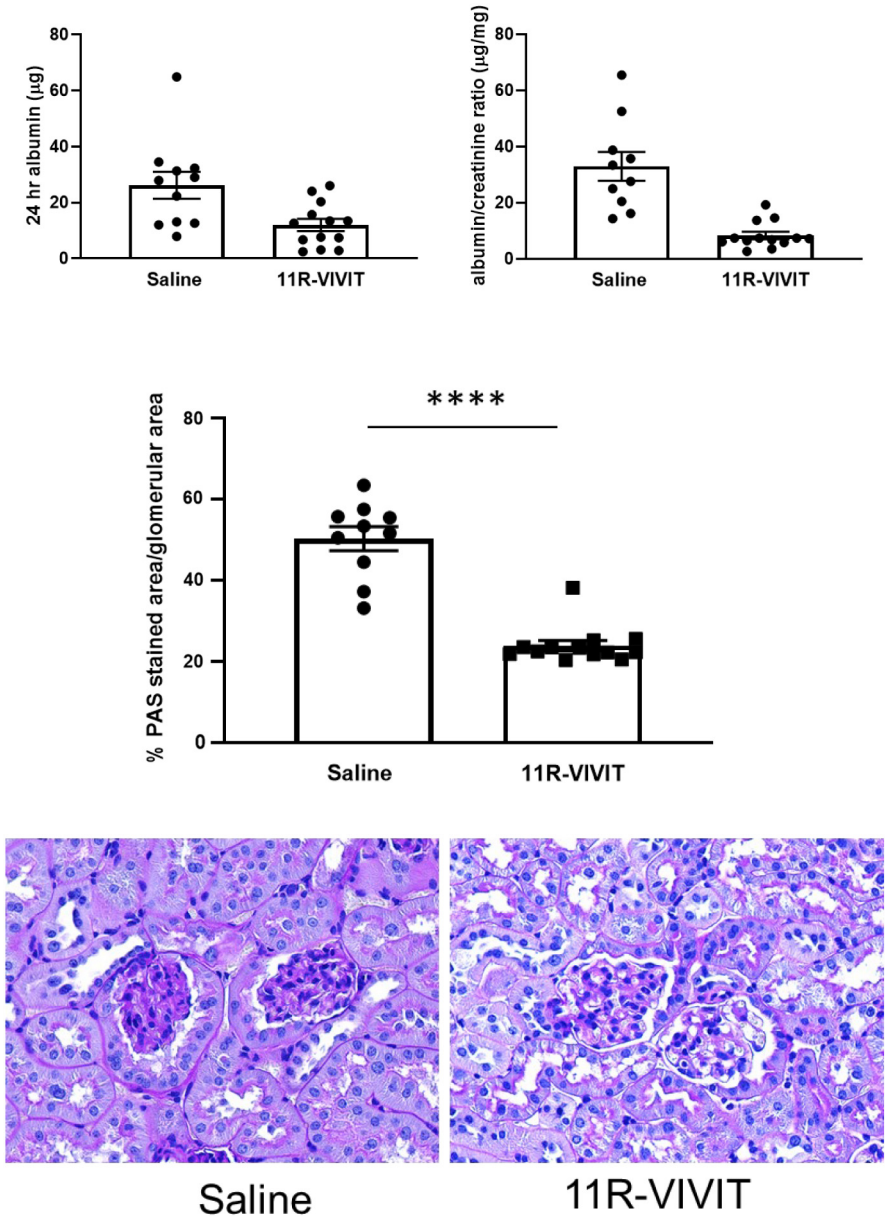

Fig. 7. The NFAT inhibitor 11R-VIVIT reduces proteinuria and renal fibrosis in diabetic mice. 7A) Urines from diabetic uninephrectomized *Calr*$^{fl/fl}$ mice treated for 8 weeks with thrice weekly intraperitoneal injections of 11R-VIVIT (1 mg/kg) or saline were analyzed for albumin in 24 h samples and the albumin/creatinine ratio. Results are the means ± SEM, (n = 10–13/group). Results were analyzed by the two-tailed, t-test with Welch's correction, *p = 0.01, ***p = 0.0009. 7B) Kidneys were harvested after 11 weeks of treatment and the percent PAS stained area/glomerular area was evaluated in 15 sections/slide (n = 10–13 animals/group). Original magnification was 40×. Results were analyzed by the two-tailed t-test with Welch's correction, ****$p < 0.0001$.

Immunoblotting

Cells were washed once with Dulbecco's PBS and total protein was isolated by lysing cells in Laemmli buffer with protease inhibitors and 5% (v/v) β-mercaptoethanol. Immunoblotting was performed using standard procedures. Membranes were blocked with 5% bovine serum albumin for 1 h at room temperature, and incubated with primary antibodies overnight at 4 °C or at room temperature for 2 h. The antibodies used were goat anti-CRT (MYBiosource, San Diego, CA, cat. No. MBS222424) (Fig. 1B) and rabbit polyclonal antibody to β-tubulin (Santa Cruz SC-9104) or rabbit monoclonal antibody to CRT (Abcam, ab108395) with rabbit monoclonal anti-GAPDH (Cell Signaling #2118) (Supplemental Fig. 1a) as a loading control. After washing three times with Tris-buffered saline

buffer containing 0.05% tween 20 (TBS-T), the membranes were incubated with secondary antibodies for 1 h and washed three times with TBS-T buffer. The immunoblots were then developed by chemiluminescence. Image J was used for densitometric analyses.

Soluble collagen assay

Treatments were initiated after cell transfection and incubation in the transfection medium overnight. Medium was changed and cells were incubated for 24 h prior to start of treatment. After 72-h of TGF-β (350 pM) or glucose (5 or 30 mM) stimulation, conditioned media were collected in microcentrifuge tubes in the presence of protease inhibitor cocktail and centrifuged at 5000 rpm for 5 min to eliminate cell debris. The Sircol™ Soluble Collagen Assay (Biocolor, UK) was used to quantify newly-synthesized, soluble collagens in conditioned media following the manufacturer's protocol. Cold Collagen Isolation and Concentration Reagent (200 µl) was added to 1 ml of each conditioned medium sample, mixed by inversion, and incubated overnight at 4 °C. Tubes were centrifuged at 12,000 rpm for 10 min and the supernatant slowly removed to avoid loss of invisible hydrated collagen pellet. Sircol Dye Reagent (1 ml) was added to each collagen pellet (dissolved in 100 µl media), as well as to collagen standards and the blank negative control. Samples were mixed by inversion and gently shaken on a mechanical shaker for 30 min. Tubes were centrifuged at 12,000 rpm for 10 min and supernatants discarded by inversion. Ice-cold Acid-Salt Wash Reagent (750 µl) was gently added to the pellet (collagen-dye complex) to remove unbound dye from the collagen-dye pellet and centrifuged at 12,000 rpm for 10 min. Tubes were carefully drained and 250 µl of Alkali Reagent was added to resolubilized the collagen-bound dye by vortexing. Sample (200 µl), standards, or blank were transferred to a 96-well plate and the absorbance was read at 540 nm using an ELISA plate reader. The concentration of soluble collagen in the conditioned media was determined from the collagen standard curve. Each measurement represents the mean of at least three separate biological experiments.

Quantitative reverse transcription-PCR (qRT-PCR) analysis

Total RNA from cells was isolated using a TRIzol Reagent (Ambion, Thermo Fisher Scientific) according to the manufacturer's protocol and treated with DNase I (Deoxyribonuclease I), (Cat. No. 18068-015, Invitrogen, Thermo Fisher Scientific) for elimination DNA during critical RNA purification. Reverse transcription was performed by using SuperScript® First-Strand Synthesis System for RT-PCR kit (Invitrogen Cat# 11904-018). Quantitative reverse-transcription PCR (qRT-PCR) was conducted on a MyiQ Single Color Real-Time PCR Detection System (Bio-Rad, Hercules, CA), using SsoAdvanced™ Universal SYBR® Green Supermix, SYBR Premix (Bio Rad #1725270) with specific primers, Amplification was initiated at 95 °C for 5 min, followed by 40 cycles of q-PCR at 95 °C for 5 s (denaturation) and at 58 °C for 30 s (annealing), and at 72 °C for 30s (extension). mRNA expression was measured from triplicate wells for each condition and mRNA levels normalized to ribosomal protein S9 were expressed as fold difference relative to the control group using the ΔΔCt method. Three to four separate experiments (biological replicates) were performed.

Calr $^{fl/fl}$ mice

All protocols were approved by the Institutional Animal Care and Use Committee at the University of Alabama at Birmingham and were consistent with the Guide for the Care and Use of Laboratory Animals published by the National Institutes of Health. CRT floxed mice on the B6D2F1 background were generated by Tokuhiro et al. [89]. Ten to 14-week-old CRT floxed mice were provided by Dr. Marek Michalak (University of Alberta) and maintained at constant humidity (60 ± 5%), temperature (24 ± 1 °C), and light cycle (6:00 A.M. to 6:00 P.M.). Mice were fed a standard pellet diet ad libitum. The presence of loxP sites in male and female breeders was confirmed by PCR [20]. Functionality of loxP sites were confirmed by using Cre-recombinase-IRES-GFP to knockout CRT in cells receiving the plasmid. Male mice were used for these studies.

Uninephrectomy

Mice underwent a left nephrectomy at 24 weeks of age. Mice were anesthetized with Ketamine 87 mg/kg/Xylazine 13 mg/kg, IP. Buprenorphine (0.2 mg/kg) was administered s.c. pre- and post-operatively as pain control. A longitudinal incision was made in the left flank, the kidney was isolated and two ligatures were placed around the renal pedicle using 4–0 silk sutures. The pedicle was cut between the two ligatures to remove the left kidney. The surgical wound was closed using 5–0 polypropylene sutures (Ethicon Inc.).

STZ-induced diabetes and blood glucose measurements

Two weeks after uninephrectomy, diabetes was induced with intraperitoneal injections of STZ (streptozotocin). Immediately prior to injection, STZ (Catalog Number S0130, Sigma, St. Louis, MO) was dissolved in 0.05 M sodium citrate buffer

(pH 4.5). Mice received injections of 40 mg/kg/day STZ solution i.p. for five consecutive days. Non-fasting blood glucose was measured in blood collected from the tail vein 2 weeks after the first STZ injection and again just prior to completion of the studies using a Blood Glucose Meter (AimStrip Plus, Germaine Laboratories). Mice with blood glucose levels ≥200 mg/dl were considered diabetic and only mice with diabetic glucose levels were included in the analyses.

Plasmid delivery via targeted ultrasound treatment with microbubble injection

Either 300 µg Cre-recombinase-IRES-GFP or 300 µg GFP plasmid in 50 µl volume, mixed with 200 µl OPTISON (GE Healthcare) microbubbles (MBs) (~1.2×10^8 MBs), were injected into the tail vein 18 days after the first STZ injection using previously established protocols [42]. Immediately following MB injection, mice were anesthetized with 3% isoflurane and an ultrasound (US) Applicator Head probe was placed on the shaved skin over the dorsal kidney area, using the following acoustic parameters: 1.0 MHz ultrasound frequency, 0.7 MPa peak negative pressure, 30 s pulse repetition period, and 2 min duration of exposure. The custom experimental ultrasound (US) (supported by UAB Small Animal Imaging Shared Facility) setup included a single element (0.75 in.) immersion transducer (Olympus, Waltham, MA) connected to a signal generator (AFG3022B, Tektronix, Beaverton, OR) and power amplifier (A075, Electronics and Innovation, Rochester, NY). The plasmid/MB mixture was injected via tail vein (i.v.) 18 days following STZ injection and this was repeated 2 weeks later.

Mouse urinary kidney injury molecule 1 (Kim-1) measurement

24 h urine samples were collected 2 and 7 days post ultrasound treatment with 0.2, 0.7, and 1.3 mPa peak negative pressure. Urine KIM-1 levels were measured using the R&D Systems (Cat# MKM100) TIM1/KIM1 ELISA kit per manufacturer's instructions.

NFAT inhibitor (11R-VIVIT) injection

Calr$^{fl/fl}$ mice underwent uninephrectomy and 20 days later were treated with STZ injections for 5 days as above. 11R-VIVIT (Millipore, Burlington, Massachusetts) treatments were started 19 days after the first STZ injection. Mice were treated with 1 mg/kg 11R-VIVIT three times per week via i.p. injection for 11 weeks. 24 h urine samples were collected 8 weeks after start of 11R-VIVIT injections. Only mice with blood glucose >200 mg/dl were included in the analyses.

Antibodies and immunohistochemistry

Periodic acid–Schiff (PAS) staining was performed by the UAB Comparative Pathology Laboratory. For immunohistochemical studies, mouse kidneys were fixed by overnight immersion in 4% paraformaldehyde–PBS at 4 °C and embedded into paraffin blocks. Tissues were sectioned at 3 µm thickness longitudinally for staining, tissue sections were deparaffinized in xylene and rehydrated in a series of descending ethanol concentrations. Two antigen retrieval methods were used for staining. For collagen IV, Collagen I, and NFAT, slides were treated with 4% pepsin (SIGMA P7125) for 40 min. For staining of phosphorylated Smad 2 and TSP-1, slides were treated with 10 mM sodium citrate buffer (pH 6.0) in a 95 °C water bath for 20 min followed by cooling for 20 min. Endogenous peroxidase activity was quenched with 1% hydrogen peroxide in PBS. Tissues were blocked with 2% normal horse serum (Sigma H0146) or with 0.2% BSA for anti-TSP-1 staining for 30 min. Slides were incubated with primary antibodies in PBS with 2% horse serum or with 0.2% BSA for anti-TSP-1 staining and 0.1% Triton X-100 overnight at 4 °C. Primary antibodies included: goat anti-type IV collagen (dilution 1:40) (Southern Biotech Cat# 1340-01 Birmingham, USA); rabbit anti-type I collagen (dilution 1:200) (Abcam Cat# ab34710 Cambridge, MA USA); rabbit anti-NFAT2 (dilution 1:70) (Abcam Cat #ab25916); mouse monoclonal anti-thrombospondin 1 (clone A4.1) (dilution 1:100), (Thermo Fisher Grand Island, NY USA); rabbit anti-phospho-Smad 2 (SER465/467) (dilution 1:50).(Millipore Burlington Massachusetts, USA); rabbit monolconal anti-CRT (1:200) (Abcam Cat#92516). Non-immune IgG served as a negative control. After washing in PBS with 0.1% Tween-20, appropriate biotinylated secondary antibodies (Vector Laboratories) were applied to the tissue for 1 h at room temperature, followed by HRP-conjugated streptavidin (ABC kit, Vector Laboratories) for 1 h at room temperature at dilutions recommended by the manufacturer. Processed sections were developed with diaminobenzidine hydrochloride (DAB) (Vector Laboratories) and then were counterstained with hematoxylin. After dehydration, the slides were mounted in Vecta-Mount mounting medium (Vector Laboratories).

Analysis of CRT in renal lysates

CRT protein levels were examined in renal lysates of kidney sections from each of the three experimental groups (n = 4/group). Mouse kidneys were lysed in RIPA buffer (Radioimmunoprecipitation assay buffer) (25 mmol/l Tris-HCl (pH 7.6), 150 mmol/l NaCl, 1% Nonidet P-40 1% sodium deoxycholate, and 0.1% SDS) containing protease inhibitor and phosphatase inhibitor (Sigma-Aldrich Corp.). Lysates were sonicated in a Sonic Dismembrator (Model 500, Fisher Scientific). Protein concentration was measured using the Pierce BCA Protein Assay kit (#23227,

ThemoFisher). Lysates (8 μg protein) were separated by SDS-polyacrylamide electrophoresis and transferred to PVDF membranes for immunoblotting as described above. Membranes were incubated with rabbit anti-CRT antibody (1:10,000 dilution, Abcam #108395, EPR3925) [42]. Densitometric analyses of bands was performed by normalizing density to total protein using the REVERT total protein stain (Li-COR, Lincoln, NE).

Morphometric analyses

All analyses were performed on slides coded to blind the user to the experimental condition. Digital images of Periodic Acid-Schiff (PAS) stained glomeruli were captured with a 40× lens using a Nikon ECLIPSE Ci (Nikon Instruments, Melville, NY) with SPOT Insight (SPOT Imaging Solutions, Sterling Heights, MI). Fifteen cortical glomeruli per slide with a similar maximal diameter and approximately equal numbers of glomerular from the outer, middle, and inner zones of the cortex were selected for analyses and PAS-stained area was calculated using MetaMorph software.

For analyses of immunostaining, images were captured using a Nikon ECLIPSE TE2000-U microscope equipped with a Cri Nuance multispectral imaging system. Images of 15 fields/slide/group were captured at 40× magnification for collagen I, collagen IV, and NFAT. Images of CRT were captured and analyzed for 6 fields/slide/group at 10× magnification. Slides from 6 animals per group were analyzed for each antigen. Images were analyzed using Nuance image-analysis software version 2.8.0 (PerkinElmer Inc., Waltham, MA), at the UAB Pediatrics Neonatology Core.

Transmission electron microscopy

Glutaraldehyde fixed cortical renal sections were processed (embedded, stained, and sectioned) by the UAB High Resolution Imaging Facility Electron Microscopy Core. Images were viewed and photographed using a FEI TECNAI T12 20-120Kv transmission electron microscope. Renal sections were examined from three animals/group for GFP MB/US and CRE MB/Us groups.

Analysis of kidney function

For 24-h urine collection, individual mice were placed in metabolic cages with access to chow and water (Thermo Fisher Scientific Inc., Rochester, NY) Urine samples were centrifuged for 10 min at 4 °C, and supernatants were stored at –80 °C until use. Urine albumin concentration was measured using a competitive enzyme-linked immunosorbent assay method (Albuwell M kit; Exocell Inc., Philadelphia, PA). Urine creatinine level was measured by the picric acid method (Creatinine Companion kit; Exocell Inc.) following the manufacturer's instructions.

Statistical analysis

All analyses were performed using GraphPad Prism version 8 with the specific analysis method indicated in the figure legend.

Supplementary data to this article can be found online at https://doi.org/10.1016/j.mbplus.2020.100034.

Declaration of competing interest

The authors have no competing or conflicting interests.

Acknowledgements

Research reported in this publication was supported by the UAB High Resolution Imaging Facility (HRIF) Electron Microscopy Core with the expert assistance of Melissa Chimento. The authors would like to thank Brian Halloran at UAB Pediatrics Neonatology Core for technical support of the light microscopy imaging system and software.

Funding sources

This work was supported by grant W81XWH-14-1-0203 from the Department of Defense to JEMU. O'Brien Core Center for AKI (NIH P30 DK079337) supported the resources for the serum creatinine studies. The UAB HRIF is supported by the National Cancer Institute Cancer Center Support Grant P30 CA013148 and by the National Institute of Arthritis, Musculoskeletal, and Skin Diseases of the National Institutes of Health under Award Number P30 AR048311.

Received 30 January 2020;
Received in revised form 13 March 2020;
Accepted 20 March 2020
Available online 3 April 2020

Keywords:
Diabetic nephropathy;
Collagen;
NFAT;
Calreticulin;
Fibrosis

Current address: A. Lu, Department of Pediatrics, University of Alabama at Birmingham, Birmingham, AL 35294, USA.
Current address: B.Y. Owusu, Clinical Chemistry Department of Laboratory Medicine, University of Washington Medical Center, Seattle, WA, 98195-71103, USA.
Current Address: A.V. Borovjagin, Department of Biomedical Engineering, University of Alabama at Birmingham, Birmingham, AL 35294-0019, USA.

Abbreviations used:
ER, endoplasmic reticulum; CRT, calreticulin; ECM, extracellular matrix; EMT, epithelial to mesenchymal transition; GRP78, glucose related protein 78; MB/US, microbubble/ultrasound; NFAT, nuclear factor of activated T cells; PAS, Periodic Acid-Schiff; 4-PBA, 4-phenylbutyrate; STZ, streptozotocin; TGF-β, transforming growth factor-β; UPR, unfolded protein response.

References

[1] M.T. Lindenmeyer, M.P. Rastaldi, M. Ikehata, M.A. Neusser, M. Kretzler, C.D. Cohen, D. Schlondorff, Proteinuria and hyperglycemia induce endoplasmic reticulum stress, Journal of the American Society of Nephrology 19 (11) (2008) 2225–2236.
[2] R. Inagi, Endoplasmic reticulum stress in the kidney as a novel mediator of kidney injury, Nephron. Experimental Nephrology 112 (1) (2009) e1–e9.
[3] M. Kitamura, Endoplasmic reticulum stress in the kidney, Clinical and Experimental Nephrology 12 (5) (2008) 317–325.
[4] A.V. Cybulsky, Endoplasmic reticulum stress in proteinuric kidney disease, Kidney International 77 (3) (2010) 187–193.
[5] L. Pereira, J. Matthes, I. Schuster, H.H. Valdivia, S. Herzig, S. Richard, A.M. Gomez, Mechanisms of [Ca2+]i transient decrease in cardiomyopathy of db/db type 2 diabetic mice, Diabetes 55 (3) (2006) 608–615.
[6] W. Qi, J. Mu, Z.F. Luo, W. Zeng, Y.H. Guo, Q. Pang, Z.L. Ye, L. Liu, F.H. Yuan, B. Feng, Attenuation of diabetic nephropathy in diabetes rats induced by streptozotocin by regulating the endoplasmic reticulum stress inflammatory response, Metabolism 60 (5) (2011) 594–603.
[7] M. Kurokawa, M. Hideshima, Y. Ishii, S. Kyuwa, Y. Yoshikawa, Aortic ER stress in streptozotocin-induced diabetes mellitus in APA hamsters, Experimental Animals 58 (2) (2009) 113–121.
[8] G. Liu, Y. Sun, Z. Li, T. Song, H. Wang, Y. Zhang, Z. Ge, Apoptosis induced by endoplasmic reticulum stress involved in diabetic kidney disease, Biochemical and Biophysical Research Communications 370 (4) (2008) 651–656.
[9] H. Liu, R.C. Bowes 3rd, B. van de Water, C. Sillence, J.F. Nagelkerke, J.L. Stevens, Endoplasmic reticulum chaperones GRP78 and calreticulin prevent oxidative stress, Ca2+ disturbances, and cell death in renal epithelial cells, The Journal of Biological Chemistry 272 (35) (1997) 21751–21759.
[10] I. Tabas, The role of endoplasmic reticulum stress in the progression of atherosclerosis, Circulation Research 107 (7) (2010) 839–850.
[11] H. Tanjore, T.S. Blackwell, W.E. Lawson, Emerging evidence for endoplasmic reticulum stress in the pathogenesis of idiopathic pulmonary fibrosis, American Journal of Physiology. Lung Cellular and Molecular Physiology 302 (8) (2012) L721–L729.
[12] H. Tanjore, D.S. Cheng, A.L. Degryse, D.F. Zoz, R. Abdolrasulnia, W.E. Lawson, T.S. Blackwell, Alveolar epithelial cells undergo epithelial-to-mesenchymal transition in response to endoplasmic reticulum stress, The Journal of Biological Chemistry 286 (35) (2011) 30972–30980.
[13] S. Lenna, M. Trojanowska, The role of endoplasmic reticulum stress and the unfolded protein response in fibrosis, Current Opinion in Rheumatology 24 (6) (2012) 663–668.
[14] J. Groenendyk, D. Lee, J. Jung, J.R. Dyck, G.D. Lopaschuk, L.B. Agellon, M. Michalak, Inhibition of the unfolded protein response mechanism prevents cardiac fibrosis, PLoS One 11 (7) (2016), e0159682.
[15] A. Burman, H. Tanjore, T.S. Blackwell, Endoplasmic reticulum stress in pulmonary fibrosis, Matrix Biology 68-69 (2018) 355–365.
[16] S.H. Liu, C.C. Yang, D.C. Chan, C.T. Wu, L.P. Chen, J.W. Huang, K.Y. Hung, C.K. Chiang, Chemical chaperon 4-phenylbutyrate protects against the endoplasmic reticulum stress-mediated renal fibrosis in vivo and in vitro, Oncotarget 7 (16) (2016) 22116–22127.
[17] H. Kim, C.H. Baek, R.B. Lee, J.W. Chang, W.S. Yang, S.K. Lee, Anti-fibrotic effect of losartan, an angiotensin II receptor blocker, is mediated through inhibition of ER stress via up-regulation of SIRT1, followed by induction of HO-1 and Thioredoxin, International Journal of Molecular Sciences 18 (2) (2017).
[18] Z. Liu, Y. Zhang, Z. Tang, J. Xu, M. Ma, S. Pan, C. Qiu, G. Guan, J. Wang, Matrine attenuates cardiac fibrosis by affecting ATF6 signaling pathway in diabetic cardiomyopathy, European Journal of Pharmacology 804 (2017) 21–30.
[19] K.Y. Tsang, D. Chan, J.F. Bateman, K.S. Cheah, In vivo cellular adaptation to ER stress: survival strategies with double-edged consequences, Journal of Cell Science 123(Pt 13) 2145–54.
[20] K.A. Zimmerman, L.V. Graham, M.A. Pallero, J.E. Murphy-Ullrich, Calreticulin regulates transforming growth factor-beta-stimulated extracellular matrix production, The Journal of Biological Chemistry 288 (20) (2013) 14584–14598.
[21] L.S. Gewin, Renal fibrosis: primacy of the proximal tubule, Matrix Biology 68–69 (2018) 248–262.
[22] M. Michalak, J. Groenendyk, E. Szabo, L.I. Gold, M. Opas, Calreticulin, a multi-process calcium-buffering chaperone of the endoplasmic reticulum, The Biochemical Journal 417 (3) (2009) 651–666.
[23] J. Groenendyk, J. Lynch, M. Michalak, Calreticulin, Ca2+, and calcineurin - signaling from the endoplasmic reticulum, Molecules and Cells 17 (3) (2004) 383–389.
[24] A.W. Orr, C.A. Elzie, D.F. Kucik, J.E. Murphy-Ullrich, Thrombospondin signaling through the calreticulin/LDL receptor-related protein co-complex stimulates random and directed cell migration, Journal of Cell Science 116 (Pt 14) (2003) 2917–2927.
[25] M.P. Fadel, E. Dziak, C.M. Lo, J. Ferrier, N. Mesaeli, M. Michalak, M. Opas, Calreticulin affects focal contact-dependent but not close contact-dependent cell-substratum adhesion, The Journal of Biological Chemistry 274 (21) (1999) 15085–15094.
[26] S. Goicoechea, A.W. Orr, M.A. Pallero, P. Eggleton, J.E. Murphy-Ullrich, Thrombospondin mediates focal adhesion

disassembly through interactions with cell surface calreticulin, The Journal of Biological Chemistry 275 (46) (2000) 36358–36368.
[27] S.J. Gardai, K.A. McPhillips, S.C. Frasch, W.J. Janssen, A. Starefeldt, J.E. Murphy-Ullrich, D.L. Bratton, P.A. Oldenborg, M. Michalak, P.M. Henson, Cell-surface calreticulin initiates clearance of viable or apoptotic cells through trans-activation of LRP on the phagocyte, Cell 123 (2) (2005) 321–334.
[28] M.A. Pallero, C.A. Elzie, J. Chen, D.F. Mosher, J.E. Murphy-Ullrich, Thrombospondin 1 binding to calreticulin-LRP1 signals resistance to anoikis, The FASEB Journal 22 (11) (2008) 3968–3979.
[29] M.T. Sweetwyne, J.E. Murphy-Ullrich, Thrombospondin1 in tissue repair and fibrosis: TGF-beta-dependent and independent mechanisms, Matrix Biology 31 (3) (2012) 178–186.
[30] L.B. Nanney, C.D. Woodrell, M.R. Greives, N.L. Cardwell, A. C. Pollins, T.A. Bancroft, A. Chesser, M. Michalak, M. Rahman, J.W. Siebert, L.I. Gold, Calreticulin enhances porcine wound repair by diverse biological effects, The American Journal of Pathology 173 (3) (2008) 610–630.
[31] M.R. Greives, F. Samra, S.C. Pavlides, K.M. Blechman, S.M. Naylor, C.D. Woodrell, C. Cadacio, J.P. Levine, T.A. Bancroft, M. Michalak, S.M. Warren, L.I. Gold, Exogenous calreticulin improves diabetic wound healing, Wound Repair and Regeneration 20 (5) (2012) 715–730.
[32] L.I. Gold, P. Eggleton, M.T. Sweetwyne, L.B. Van Duyn, M.R. Greives, S.M. Naylor, M. Michalak, J.E. Murphy-Ullrich, Calreticulin: non-endoplasmic reticulum functions in physiology and disease, The FASEB Journal 24 (3) (2010) 665–683.
[33] B.Y. Owusu, K.A. Zimmerman, J.E. Murphy-Ullrich, The role of the endoplasmic reticulum protein calreticulin in mediating TGF-beta-stimulated extracellular matrix production in fibrotic disease, Journal of Cell Communication and Signaling 12 (1) (2018) 289–299.
[34] S. Papp, M.P. Fadel, H. Kim, C.A. McCulloch, M. Opas, Calreticulin affects fibronectin-based cell-substratum adhesion via the regulation of c-Src activity, The Journal of Biological Chemistry 282 (22) (2007) 16585–16598.
[35] S. Papp, E. Szabo, H. Kim, C.A. McCulloch, M. Opas, Kinase-dependent adhesion to fibronectin: regulation by calreticulin, Experimental Cell Research 314 (6) (2008) 1313–1326.
[36] L. Van Duyn Graham, M.T. Sweetwyne, M.A. Pallero, J.E. Murphy-Ullrich, Intracellular calreticulin regulates multiple steps in fibrillar collagen expression, trafficking, and processing into the extracellular matrix, The Journal of Biological Chemistry 285 (10) (2010) 7067–7078.
[37] E. Szabo, S. Papp, M. Opas, Differential calreticulin expression affects focal contacts via the calmodulin/CaMK II pathway, Journal of Cellular Physiology 213 (1) (2007) 269–277.
[38] X. Fan, Y. Yao, Y. Zhang, Calreticulin promotes proliferation and extracellular matrix expression through notch pathway in cardiac fibroblasts, Advances in Clinical and Experimental Medicine 27 (7) (2018) 887–892.
[39] F. Karimzadeh, M. Opas, Calreticulin is required for TGF-beta-induced epithelial-to-mesenchymal transition during Cardiogenesis in mouse embryonic stem cells, Stem Cell Reports 8 (5) (2017) 1299–1311.
[40] Y. Wu, X. Xu, L. Ma, Q. Yi, W. Sun, L. Tang, Calreticulin regulates TGF-beta1-induced epithelial mesenchymal transition through modulating Smad signaling and calcium signaling, The International Journal of Biochemistry & Cell Biology 90 (2017) 103–113.
[41] N. Prakoura, P.K. Politis, Y. Ihara, M. Michalak, A.S. Charonis, Epithelial calreticulin up-regulation promotes profibrotic responses and tubulointerstitial fibrosis development, The American Journal of Pathology 183 (5) (2013) 1474–1487.
[42] K.A. Zimmerman, D. Xing, M.A. Pallero, A. Lu, M. Ikawa, L. Black, K.L. Hoyt, J.H. Kabarowski, M. Michalak, J.E. Murphy-Ullrich, Calreticulin regulates neointima formation and collagen deposition following carotid artery ligation, Journal of Vascular Research 52 (5) (2015) 306–320.
[43] X. Liu, J. Shen, R. Zhan, X. Wang, Z. Zhang, X. Leng, Z. Yang, L. Qian, Proteomic analysis of homocysteine induced proliferation of cultured neonatal rat vascular smooth muscle cells, Biochimica et Biophysica Acta 1794 (2) (2009) 177–184.
[44] M.T. Núñez, A. Osorio, V. Tapia, A. Vergara, C.V. Mura, Iron-induced oxidative stress up-regulates calreticulin levels in intestinal epithelial (Caco-2) cells, Journal of Cellular Biochemistry 82 (4) (2001) 660–665.
[45] L. Jia, M. Xu, W. Zhen, X. Shen, Y. Zhu, W. Wang, X. Wang, Novel anti-oxidative role of calreticulin in protecting A549 human type II alveolar epithelial cells against hypoxic injury, American Journal of Physiology. Cell Physiology 294 (1) (2008) C47–C55.
[46] M. Waser, N. Mesaeli, C. Spencer, M. Michalak, Regulation of calreticulin gene expression by calcium, The Journal of Cell Biology 138 (3) (1997) 547–557.
[47] R. Heal, J. McGivan, Induction of calreticulin expression in response to amino acid deprivation in Chinese hamster ovary cells, The Biochemical Journal 329 (Pt 2) (1998) 389–394.
[48] K.P. Kypreou, P. Kavvadas, P. Karamessinis, M. Peroulis, A. Alberti, P. Sideras, S. Psarras, Y. Capetanaki, P.K. Politis, A. S. Charonis, Altered expression of calreticulin during the development of fibrosis, Proteomics 8 (12) (2008) 2407–2419.
[49] J. Klein, S. Jupp, P. Moulos, M. Fernandez, B. Buffin-Meyer, A. Casemayou, R. Chaaya, A. Charonis, J.L. Bascands, R. Stevens, J.P. Schanstra, The KUPKB: a novel web application to access multiomics data on kidney disease, The FASEB Journal 26 (5) (2012) 2145–2153.
[50] H. Dihazi, G.H. Dihazi, C. Mueller, L. Lahrichi, A.R. Asif, A. Bibi, M. Eltoweissy, R. Vasko, G.A. Mueller, Proteomics characterization of cell model with renal fibrosis phenotype: osmotic stress as fibrosis triggering factor, Journal of Proteomics 74 (3) (2011) 304–318.
[51] A. Giorgi, I. Tempera, G. Napoletani, D. Drovandi, C. Potesta, S. Martire, E. Mandosi, T. Filardi, M. Eugenia Schinina, S. Morano, M. d'Erme, B. Maras, Poly(ADP-ribosylated) proteins in mononuclear cells from patients with type 2 diabetes identified by proteomic studies, Acta Diabetologica 54 (9) (2017) 833–842.
[52] G. Boden, X. Duan, C. Homko, E.J. Molina, W. Song, O. Perez, P. Cheung, S. Merali, Increase in endoplasmic reticulum stress-related proteins and genes in adipose tissue of obese, insulin-resistant individuals, Diabetes 57 (9) (2008) 2438–2444.
[53] A.T. Sage, S. Holtby-Ottenhof, Y. Shi, S. Damjanovic, A.M. Sharma, G.H. Werstuck, Metabolic syndrome and acute hyperglycemia are associated with endoplasmic reticulum stress in human mononuclear cells, Obesity (Silver Spring) 20 (4) (2012) 748–755.
[54] A.L. Cardoso, A. Fernandes, J.A. Aguilar-Pimentel, M.H. de Angelis, J.R. Guedes, M.A. Brito, S. Ortolano, G. Pani, S. Athanasopoulou, E.S. Gonos, M. Schosserer, J. Grillari, P.

Peterson, B.G. Tuna, S. Dogan, A. Meyer, R. van Os, A.U. Trendelenburg, Towards frailty biomarkers: candidates from genes and pathways regulated in aging and age-related diseases, Ageing Research Reviews 47 (2018) 214–277.
[55] H. Totary-Jain, T. Naveh-Many, Y. Riahi, N. Kaiser, J. Eckel, S. Sasson, Calreticulin destabilizes glucose transporter-1 mRNA in vascular endothelial and smooth muscle cells under high-glucose conditions, Circulation Research 97 (10) (2005) 1001–1008.
[56] Y. Riahi, Y. Sin-Malia, G. Cohen, E. Alpert, A. Gruzman, J. Eckel, B. Staels, M. Guichardant, S. Sasson, The natural protective mechanism against hyperglycemia in vascular endothelial cells: roles of the lipid peroxidation product 4-hydroxydodecadienal and peroxisome proliferator-activated receptor delta, Diabetes 59 (4) (2010) 808–818.
[57] A.T. Sage, L.A. Walter, Y. Shi, M.I. Khan, H. Kaneto, A. Capretta, G.H. Werstuck, Hexosamine biosynthesis pathway flux promotes endoplasmic reticulum stress, lipid accumulation, and inflammatory gene expression in hepatic cells, American Journal of Physiology. Endocrinology and Metabolism 298 (3) (2010) E499–E511.
[58] V. Srinivasan, U. Tatu, V. Mohan, M. Balasubramanyam, Molecular convergence of hexosamine biosynthetic pathway and ER stress leading to insulin resistance in L6 skeletal muscle cells, Molecular and Cellular Biochemistry 328 (1–2) (2009) 217–224.
[59] Y. Sun, Q. Wang, Y. Fang, C. Wu, G. Lu, Z. Chen, Activation of the Nkx2.5-Calr-p53 signaling pathway by hyperglycemia induces cardiac remodeling and dysfunction in adult zebrafish, Disease models & mechanisms 10 (10) (2017) 1217–1227.
[60] J.H. Ma, S. Shen, J.J. Wang, Z. He, A. Poon, J. Li, J. Qu, S.X. Zhang, Comparative proteomic analysis of the mitochondria-associated ER membrane (MAM) in a long-term type 2 diabetic rodent model, Scientific Reports 7 (1) (2017) 2062.
[61] B. Yan, Y. Gan, F. Cao, Calreticulin is involved in diabetic nephropathy through inducing epithelial mesenchymal transition, Advances in Biology and Medicine 3 (2) (2018) 18–30.
[62] J.E. Murphy-Ullrich, M.J. Suto, Thrombospondin-1 regulation of latent TGF-beta activation: a therapeutic target for fibrotic disease, Matrix Biology 68–69 (2018) 28–43.
[63] M. Uil, A.M.L. Scantlebery, L.M. Butter, P.W.B. Larsen, O.J. de Boer, J.C. Leemans, S. Florquin, J. Roelofs, Combining streptozotocin and unilateral nephrectomy is an effective method for inducing experimental diabetic nephropathy in the 'resistant' C57Bl/6J mouse strain, Scientific Reports 8 (1) (2018) 5542.
[64] F. Cevikbas, L. Schaefer, P. Uhlig, H. Robenek, G. Theilmeier, F. Echtermeyer, P. Bruckner, Unilateral nephrectomy leads to up-regulation of syndecan-2- and TGF-beta-mediated glomerulosclerosis in syndecan-4 deficient male mice, Matrix Biology 27 (1) (2008) 42–52.
[65] S. Shu, J. Zhu, Z. Liu, C. Tang, J. Cai, Z. Dong, Endoplasmic reticulum stress is activated in post-ischemic kidneys to promote chronic kidney disease, EBioMedicine 37 (2018) 269–280.
[66] V.S. Vaidya, V. Ramirez, T. Ichimura, N.A. Bobadilla, J.V. Bonventre, Urinary kidney injury molecule-1: a sensitive quantitative biomarker for early detection of kidney tubular injury, American Journal of Physiology. Renal Physiology 290 (2) (2006) F517–F529.
[67] T. Ichimura, C.C. Hung, S.A. Yang, J.L. Stevens, J.V. Bonventre, Kidney injury molecule-1: a tissue and urinary biomarker for nephrotoxicant-induced renal injury, American Journal of Physiology. Renal Physiology 286 (3) (2004) F552–F563.
[68] P. Fioretto, M. Mauer, Histopathology of diabetic nephropathy, Seminars in Nephrology 27 (2) (2007) 195–207.
[69] A. Pozzi, P.D. Yurchenco, R.V. Iozzo, The nature and biology of basement membranes, Matrix Biology 57-58 (2017) 1–11.
[70] N. Mesaeli, K. Nakamura, E. Zvaritch, P. Dickie, E. Dziak, K. H. Krause, M. Opas, D.H. MacLennan, M. Michalak, Calreticulin is essential for cardiac development, The Journal of Cell Biology 144 (5) (1999) 857–868.
[71] J.L. Gooch, Y. Gorin, B.X. Zhang, H.E. Abboud, Involvement of calcineurin in transforming growth factor-beta-mediated regulation of extracellular matrix accumulation, The Journal of Biological Chemistry 279 (15) (2004) 15561–15570.
[72] J.L. Gooch, J.L. Barnes, S. Garcia, H.E. Abboud, Calcineurin is activated in diabetes and is required for glomerular hypertrophy and ECM accumulation, American Journal of Physiology. Renal Physiology 284 (1) (2003) F144–F154.
[73] L. Zhang, R. Li, W. Shi, X. Liang, S. Liu, Z. Ye, C. Yu, Y. Chen, B. Zhang, W. Wang, Y. Lai, J. Ma, Z. Li, X. Tan, NFAT2 inhibitor ameliorates diabetic nephropathy and podocyte injury in db/db mice, British Journal of Pharmacology 170 (2) (2013) 426–439.
[74] Y. Wang, G. Jarad, P. Tripathi, M. Pan, J. Cunningham, D.R. Martin, H. Liapis, J.H. Miner, F. Chen, Activation of NFAT signaling in podocytes causes glomerulosclerosis, Journal of the American Society of Nephrology 21 (10) (2010) 1657–1666.
[75] M. Naesens, D.R. Kuypers, M. Sarwal, Calcineurin inhibitor nephrotoxicity, Clinical Journal of the American Society of Nephrology 4 (2) (2009) 481–508.
[76] M.H. Roehrl, S. Kang, J. Aramburu, G. Wagner, A. Rao, P.G. Hogan, Selective inhibition of calcineurin-NFAT signaling by blocking protein-protein interaction with small organic molecules, Proceedings of the National Academy of Sciences of the United States of America 101 (20) (2004) 7554–7559.
[77] C. Yin, N. Wang, Kidney injury molecule-1 in kidney disease, Renal Failure 38 (10) (2016) 1567–1573.
[78] S.L. Cobbs, J.L. Gooch, NFATc is required for TGFbeta-mediated transcriptional regulation of fibronectin, Biochemical and Biophysical Research Communications 362 (2) (2007) 288–294.
[79] R. Li, L. Zhang, W. Shi, B. Zhang, X. Liang, S. Liu, W. Wang, NFAT2 mediates high glucose-induced glomerular podocyte apoptosis through increased Bax expression, Experimental Cell Research 319 (7) (2013) 992–1000.
[80] H. Lin, Y.M. Sue, Y. Chou, C.F. Cheng, C.C. Chang, H.F. Li, C.C. Chen, S.H. Juan, Activation of a nuclear factor of activated T-lymphocyte-3 (NFAT3) by oxidative stress in carboplatin-mediated renal apoptosis, British Journal of Pharmacology 161 (7) (2010) 1661–1676.
[81] S. Jalali, M. Aghasi, B. Yeganeh, N. Mesaeli, Calreticulin regulates insulin receptor expression and its downstream PI3 kinase/Akt signalling pathway, Biochimica et Biophysica Acta 1783 (12) (2008) 2344–2351.
[82] R. Van Krieken, N. Mehta, T. Wang, M. Zheng, R. Li, B. Gao, E. Ayaub, K. Ask, J.C. Paton, A.W. Paton, R.C. Austin, J.C. Krepinsky, Cell surface expression of 78 kDa glucose regulated protein (GRP78) mediates diabetic nephropathy, The Journal of Biological Chemistry 294 (2019) 7755–7768.
[83] C. Ji, N. Kaplowitz, M.Y. Lau, E. Kao, L.M. Petrovic, A.S. Lee, Liver-specific loss of glucose-regulated protein 78 perturbs the unfolded protein response and exacerbates a spectrum of liver diseases in mice, Hepatology 54 (1) (2011) 229–239.

[84] C.K. Chiang, S.P. Hsu, C.T. Wu, J.W. Huang, H.T. Cheng, Y. W. Chang, K.Y. Hung, K.D. Wu, S.H. Liu, Endoplasmic reticulum stress implicated in the development of renal fibrosis, Molecular Medicine 17 (11–12) (2011) 1295–1305.
[85] M.S. Razzaque, M.A. Hossain, S. Kohno, T. Taguchi, Bleomycin-induced pulmonary fibrosis in rat is associated with increased expression of collagen-binding heat shock protein (HSP) 47, Virchows Archiv 432 (5) (1998) 455–460.
[86] S. Ito, K. Nagata, Roles of the endoplasmic reticulum-resident, collagen-specific molecular chaperone Hsp47 in vertebrate cells and human disease, The Journal of Biological Chemistry 294 (6) (2019) 2133–2141.
[87] A.S. Charonis, M. Michalak, J. Groenendyk, L.B. Agellon, Endoplasmic reticulum in health and disease: the 12th International Calreticulin Workshop, Delphi, Greece, Journal of Cellular and Molecular Medicine 21 (12) (2017) 3141–3149.
[88] P. Eggleton, E. Bremer, E. Dudek, M. Michalak, Calreticulin, a therapeutic target? Expert Opinion on Therapeutic Targets 20 (9) (2016) 1137–1147.
[89] K. Tokuhiro, Y. Satouh, K. Nozawa, A. Isotani, Y. Fujihara, Y. Hirashima, H. Matsumura, K. Takumi, T. Miyano, M. Okabe, A.M. Benham, M. Ikawa, Calreticulin is required for development of the cumulus oocyte complex and female fertility, Scientific Reports 5 (2015) 14254.